Aus dem Department für Biomedizinische Wissenschaften
der Veterinärmedizinischen Universität Wien

Institut für Pharmakologie und Toxikologie
(LeiterIn: Univ.-Prof. Dr.med.univ. Veronika Sexl)

Targeting FLT3 for the Treatment of Acute Myeloid Leukemia: Chimeric Antigen Receptor (CAR) T cells versus Bispecific T cell Engager (BITE®)

Masterarbeit

Veterinärmedizinische Universität Wien

vorgelegt von

Helena Stadler

Wien, im August 2021

Interne Betreuerin:

Mag[a] rer.nat. Dagmar Gotthardt, PhD

Institut für Pharmakologie und Toxikologie
Veterinärmedizinische Universität Wien

Externen Betreuer:

Prof. Dr. Marion Subklewe
Lisa Rohrbacher, M.Sc.

Gene Center
Laboratory for Translational Cancer Immunology
Ludwig-Maximilians-Universität München

Begutachter

Univ.-Prof. Dr.rer.nat. Florian Grebien

Institut für Medizinische Biochemie
Veterinärmedizinische Universität Wien

Table of Contents

1 Introduction

1.1 Leukemia and its challenges

The hematopoietic system with all its different blood cell types (lineages) arises from hematopoietic stem cells (HSCs). HSCs reside mainly in the bone marrow (BM), harbor long-term self-renewal and differentiation potential and differentiate into a cascade of progenitor cell stages. With every differentiation step, progenitor cells continuously lose their multilineage potential and become lineage-restricted progenitors with limited capacity to divide (Rieger and Schroeder 2012). Thereby, multipotent progenitors differentiate into oligopotent common-lymphoid progenitors, that give rise to lymphocytes including T cells, B cells and NK cells and to common-myeloid progenitors that can further differentiate into various granulocytes, macrophages, monocytes, and dendritic cells as well as into erythrocytes and megakaryocytes, that give rise to platelets (Zhang et al. 2019).

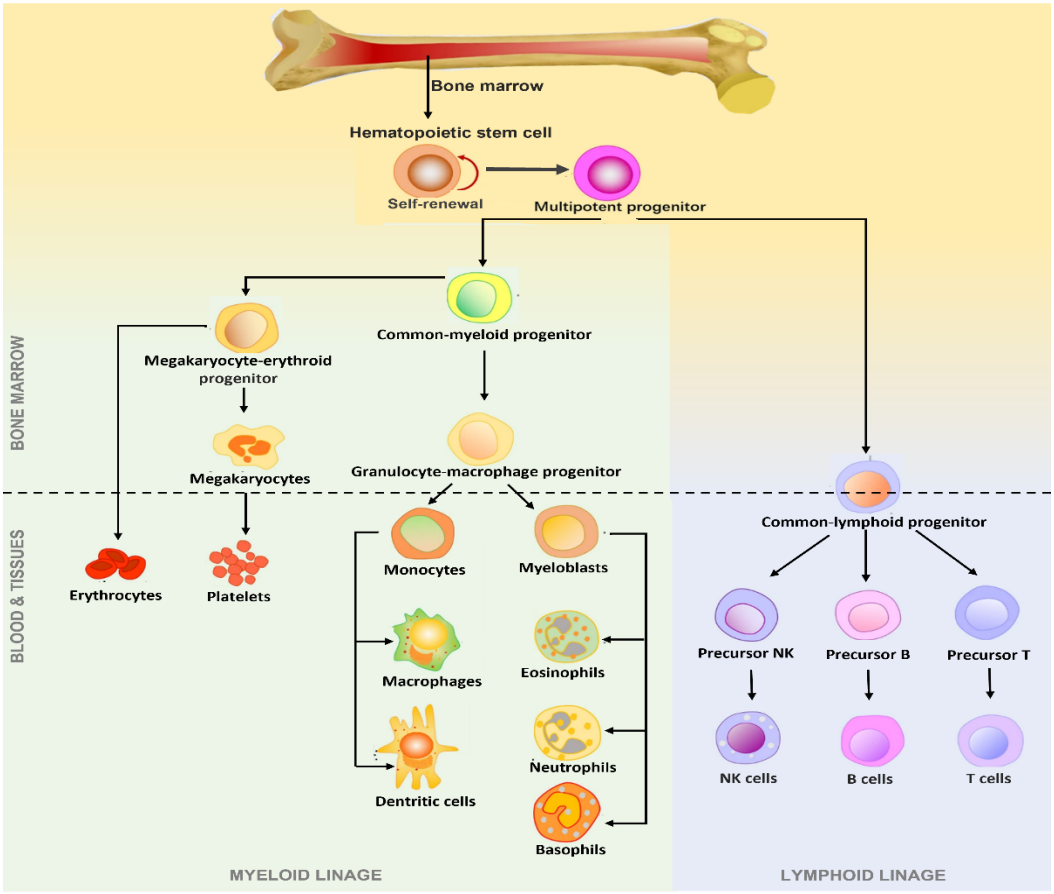

Figure 1: The hierarchical system model of hematopoietic stem cell (HSC) self-renewal and differentiation. HSCs are at the apex of the hierarchy and give rise to multipotent progenitors, that further differentiate into lymphoid or myeloid linage cells. (Figure adapted from Zhang et al. (2019))

Leukemia is the common name for several malignant hematologic disorders, which are associated with an increased number of primitive or atypical leukocytes in bone marrow and blood. As in other types of cancer, the reason for the development of malignant cells is the accumulation of mutations that disrupt the regulation of cell differentiation, division or death (Juliusson and Hough 2016). Leukemic cells can thereby arise from partially differentiated precursor cells, also called blasts, derived from both lymphoid and myeloid linage of the hematopoietic system (Chao et al. 2008). Leukemias are classified based on the present predominant cell type and the degree of cellular differentiation. Acute leukemias are characterized by a rapid clonal expansion of immature leukocytes with a fast disease progression that requires immediate treatment. Chronic leukemias are characterized by an excessive buildup of relatively mature, abnormal leukocytes with a slow disease progression. The most common leukemia types are chronic lymphocytic leukemia (CLL), chronic myelogenous leukemia (CML), acute lymphoblastic leukemia (ALL) and acute myeloid leukemia (AML) (National Cancer Institute, Thesaurus (NCIt) Code: C3161).

Since this thesis addresses the treatment of AML, this type of leukemia will be discussed in more detail below. The incidence of AML increases with age, and it is the most common acute leukemia in adults. Risk factors are underlying hematological disorders, Down syndrome, as well as prior DNA-damaging therapies with topoisomerase II-inhibitors, alkylating agents, or radiation for a previous malignant disorder. Yet in the majority of cases, AML appears as a *de novo* disease due to genetic alterations in previously healthy individuals (Juliusson and Hough 2016, De Kouchkovsky and Abdul-Hay 2016). Examples for these genetic abnormalities are chromosomal translocations, that result in the formation of chimeric fusion proteins. Accumulation of malignant, partially differentiated myeloid cells within the bone marrow, peripheral blood and infrequently in other organs are clinical manifestations of AML. Therefore, the diagnosis of AML is made by either the presence of ≥20 % blasts in the peripheral blood or bone marrow or regardless of blast count by the presence of unique genetic abnormalities like chromosomal translocations found in bone marrow cells (Juliusson and Hough 2016, De Kouchkovsky and Abdul-Hay 2016, Pelcovits and Niroula 2020). Common complaints of patients suffering from AML are fatigue, weight loss, anorexia and signs of bone marrow failure such as anemia and thrombocytopenia. Infections, disseminated intravascular coagulation and bleeding are further symptomatic complications (De Kouchkovsky and Abdul-Hay 2016, Pelcovits and Niroula 2020). Treatment of AML involves an initial induction therapy, using cytotoxic chemotherapy or hypomethylating agents to achieve complete remission (CR) with

preferably no measurable residual disease (MRD). Standard chemotherapy with cytarabine and an anthracycline lead to a CR rate of around 80 % in patients below 60 years of age, and around 60 % in patients between 60 and 70 years. MRD often persists in CR, wherefor post-remission therapy is needed to prevent relapse. Strategies for these consolidation therapies are either an additional chemotherapy or allogenic hematopoietic stem cell transplantation (allo-HSCT). Allo-HSCT, however also involves the risk of treatment-related mortality because of chronic graft versus host disease, infection from chronic immunosuppression or secondary malignancies. Further, because of concomitant comorbidities chemotherapy and transplantation are not suitable for elderly patients who account for the majority of newly diagnosed cases (Juliusson and Hough 2016, De Kouchkovsky and Abdul-Hay 2016, Pelcovits and Niroula 2020). Overall, long-term survival of AML patients remains poor, with an estimated 5-year survival rate of 28 % (Sommer et al. 2020).

1.2 The history of immunotherapy

The concept of immunotherapy goes back to William B. Coley in the late 19th century, who observed, that a bacterial infection can stimulate an immune response against tumors (Strohl and Naso 2019). However, due to the tumor cells' ability to avoid recognition and elimination by the immune system, immunotherapies achieved only limited clinical efficacy, wherefor surgery, chemo- and radiotherapy were adopted as alternative standard treatments over the years. As the understanding of the key mediators of the immune system progressed, new possibilities for immunotherapy were created (Yang 2015, Esfahani et al. 2020). A first approach to make use of these newly discovered key mediators, also known as cytokines, were high-dose interleukin 2 or interferon treatments for cancer therapy, but significant adverse events often counterbalanced modest successes. The mechanisms of immune surveillance and how innate immune cells eliminate cancer cells propelled the field of immuno-oncology into its current era (Esfahani et al. 2020). To activate antitumor immunity, a tumor–immune system interface is required which depends on some critical aspects. These first involve processing and presentation of antigens released by the tumor cells by antigen-presenting cells (APCs). Second, interaction with T lymphocytes and T-cell activation is required (Munhoz and Postow 2016). Therefore, T cells need two activating signals to become fully functional. "Signal 1" is the presentation of an antigen by major histocompatibility complex (MHC) molecules on the APCs to the corresponding T-cell receptor (TCR) on naive T cells. "Signal 2" is a costimulatory signal, which can be provided by a variety of ligands on the target cell or APC, including a B7 ligand (CD80 or CD86) interacting with CD28, OX40L with OX40 or CD70

with CD27 on T cells (Oiseth and Aziz 2017, Strohl and Naso 2019). A third critical aspect involves antigen-specific effector cell trafficking, and target tumor cell engagement of these activated effector T cell (Munhoz and Postow 2016). Upon engagement, T cells secrete cytolytic proteins (including granzymes and perforin), that form pores in target cells and elicit apoptosis. More delayed, TCR engagement induces the expression of TNF superfamily ligands on the T-cell surface that bind to cell surface death receptors (including FAS) on target cell and also induce caspase-driven apoptosis of these cells (Ross et al. 2017).

To avoid healthy tissue damage from autoimmunity, the activation of T cells is tightly regulated by inhibitory checkpoint molecules, including lymphocyte-activated-gene-3 (LAG-3), and T-cell-immunoglobulin-and-mucin-domain-containing-protein-3 (TIM3). The most attention in recent years was received by the immune checkpoint molecules programmed-cell-death-protein-1 (PD-1) and the cytotoxic T-lymphocyte-associatedantigen-4 (CTLA-4). PD-1 ligand (PD-L1) can be expressed on many cell types to protect these cells from T-cell attack. Tumor cells can exploit these T-cell inhibitory mechanisms of the PD-1/PD-L1 axis by expressing PD-L1 as an adaptive immune resistance mechanism (Oiseth and Aziz 2017). The invention of monoclonal antibodies (mAb) against the inhibitory immune checkpoints CTLA-4 and PD-1 has resulted in dramatic anti-tumor responses and numerous other agonistic or inhibitory checkpoints, for example CD28 antibodies are in clinical trials. However, immune related adverse events including immune activation and inflammatory response against the host's healthy tissues leads to limitations of these therapies (Esfahani et al. 2020).

Recently, various therapeutic strategies seek to harness the antigen-specific killing power of T cells. This thesis focuses on two of these T cell-based therapeutic strategies, namely chimeric antigen receptor (CAR)-T cells and a bispecific T-cell engager (BiTE®), which aim to direct cytotoxic T lymphocytes to specific surface antigens on cancer cells. The goal is to facilitate a polyclonal T-cell response to tumor antigens (Slaney et al. 2018).

1.3 The role of tumor associated antigens in immunotherapy with a specific focus on FLT3

Like many other cancer cells, AML cells display tumor-associated antigens (TAA) that can trigger anti-leukemia immune response. Peptides derived from these antigens are naturally processed and presented by MHC molecules, that are then recognized by T cells via their TCR, and thus exhibit target-specific immune response (Maruta et al. 2019, Anguille et al. 2012). Since one well-known immune escape mechanism, which allows the tumor cells to

avoid the recognition and killing by T cells is the downregulation or loss of MHC molecules, todays research strives for MHC-independent T cell-based therapeutic strategies (Strohl and Naso 2019). Antigen-directed immunotherapy approaches are based on TAAs expressed on the surface of tumor cells. These can either be 'active' specific immunotherapies, including CAR-T cells, BiTEs® or vaccines or 'passive' immunotherapies including allo-HSCT or donor lymphocyte infusions that are based on adoptive transfer of antigen-reactive T cells (Anguille et al. 2012). To be seen as a suitable target for therapeutic applications, TAAs should meet several criteria that were evaluated by the translational research working group of the National Cancer Institute. Applying these criteria in the context of leukemia, antigens should meet the following requirements: they should demonstrate clinical utility (a: therapeutic function), possess strong immunogenic properties (b: immunogenicity), play a defined oncogenic role (c: role of the antigen in oncogenicity), be expressed in leukemic cells with minimal to no expression in normal tissues (d: specificity) and display high and homogeneous expression levels in most to all leukemic cells, including leukemic stem cells (e: expression level, f: stem cell expression) (Cheever et al. 2009, Anguille et al. 2012). A distinction can be made between leukemia-associated antigens (LAAs) and leukemia-specific antigens (LSAs), where LSAs are seen as more appropriate targets because of their leukemia-restricted expression pattern. The category of LSAs includes unique leukemia-specific fusion proteins that arise from defined chromosomal translocations, as for example t(8;21) creating AML1-ETO, t(6;9) creating DEK-CAN and t(15;17) creating PML-RARα fusion protein. Further, leukemia-specific proteins occur due to gene mutations in leukemic cells, including mutations in the nucleophosmin 1 (NPM1) gene and internal tandem duplications (ITD) in the FMS-like tyrosine kinase 3 gene (FLT3). In contrast, LAAs are overexpressed in AML cells, but they do not result in a mutated protein. LAAs are expressed by both normal and leukemic cells, wherefore targeting LAAs, can lead to on-target toxicity and autoimmunity against healthy tissues (Anguille et al. 2012).

In this project, FLT3 was used as a target, wherefor the role of FLT3 in AML is discussed in more detail hereinafter. FLT3 (or CD135) is a transmembrane ligand-activated type 3 receptor tyrosine kinase, that plays an important role in the expansion of multipotent progenitors within the bone marrow, making it a candidate driver of leukemogenesis (Kennedy and Smith 2020, Ambinder and Levis 2021). Upon binding of an extracellular FLT3 ligand, receptor homodimerization and autophosphorylation take place to trigger FLT3 kinase activity (Figure 2). Signals for cell survival, proliferation, and differentiation are further transduced via the RAS/MAPK, JAK/STAT5 and PI3K/AKT pathways (Daver et al. 2019, Ambinder and Levis

2021). FLT3 is expressed by a limited subset of hematopoietic stem cells, multipotent progenitors, common lymphoid progenitors, common myeloid progenitors, and mature dendritic cells in healthy individuals (Brauchle et al. 2020, Tsapogas et al. 2017). FLT3 is mutated in approximately 30 % of newly diagnosed AML cases and can either occur as ITDs (≈25 %) or as point mutations in the tyrosine kinase domain (TKD) (7–10 %) (Daver et al. 2019, Ambinder and Levis 2021). FLT3-ITDs are in-frame duplications that can be located within the receptor's autoinhibitory juxtamembrane and/or the TK1 domain. With 3 to >1,000 nucleotides, the size of these duplications can vary a lot. FLT3-ITD or FLT3-TKD both lead to the constitutive activation of the FLT3 kinase and its downstream pathways, resulting in proliferation and survival of AML cells (Daver et al. 2019, Kennedy and Smith 2020). However, FLT3 is a potential driver of leukemogenesis also regardless of these two mutation types. Even when no FLT3 coding mutation is detectable, the receptor can contribute to the survival and proliferation by overexpression on the cell surface of leukemic blasts (Ambinder and Levis 2021).

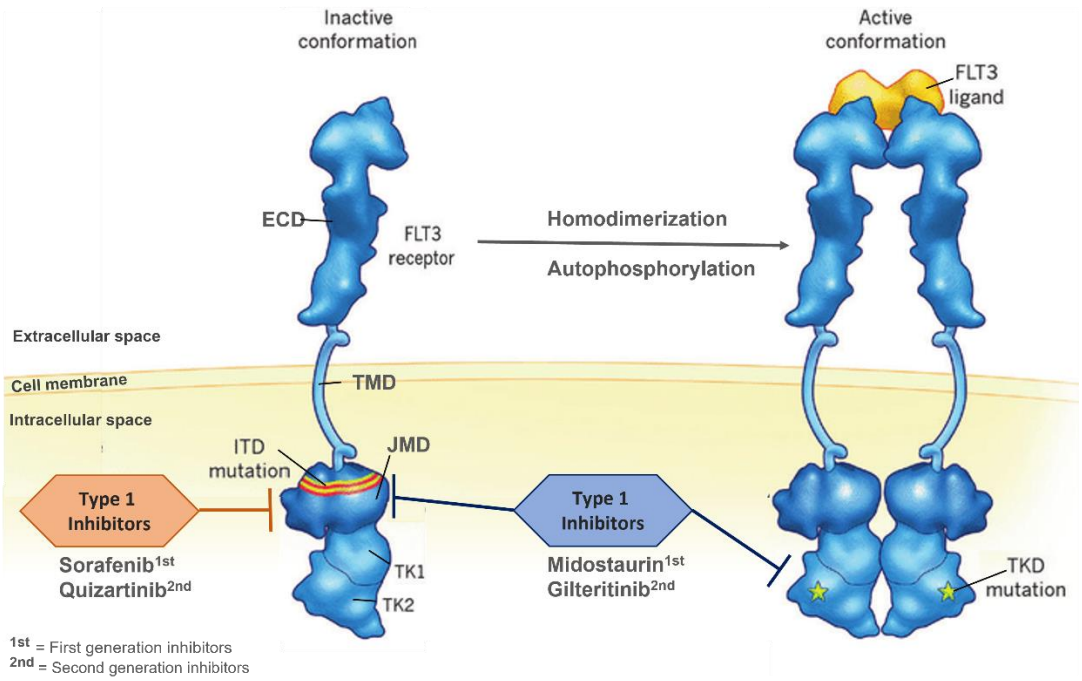

Figure 2: FMS-like tyrosine kinase 3 (FLT3) and tyrosine kinase inhibitors (TKIs). FLT3 receptor consisting of an extracellular ligand-binding domain (ECD), a transmembrane domain (TMD), juxtamembrane domain (JMD) and two tyrosine kinase domains (TK1, TK2). Upon ligand binding, homodimerization of the receptor takes place. Internal tandem duplications (ITD) in the JMD and point mutations in the tyrosine kinase domain (TKD) are the most frequent mutations. Type I TKIs inhibit both FLT3-TKD and FLT3-ITD, while type II TKIs only inhibit FLT3-ITD. Second-generation FLT3 inhibitors (^{2nd}) have a higher specificity for FLT3. (Figure adapted from: Daver et al. (2019))

Clinically, FLT3-ITD mutated AML is linked to higher relapse rates and inferior overall survival. Moreover, high allelic ratios go along with higher disease risk and high leukemic burden, conferring a poor prognosis. Further, FLT3-ITD mutation directly or indirectly lead to a selective growth advantage in a clone at relapse, wherefor 75 % of patients with FLT3-ITD–mutated AML at diagnosis continue to have the ITD mutation at relapse (Daver et al. 2019, Kennedy and Smith 2020). Several small-molecule tyrosine kinase inhibitors (TKI) targeting FLT3 have been developed to face the poor prognosis for AML patients with mutated FLT3. These TKIs demonstrated a substantial clinical benefit in the relapsed/refractory AML setting in combination with chemotherapy. First-generation multi-kinase inhibitors (including sorafenib and midostaurin) target FLT3 as well as certain other kinases which can lead to toxicities due to multiple off-target effects. Less toxic effects are accomplished with second generation inhibitors (including quizartinib and gilteritinib), which are more potent and show higher specificity for FLT3. TKIs can further be divided in type I inhibitors (gilteritinib, midostaurin), inhibiting both FLT3-TKD and FLT3-ITD because they bind the receptor in the active conformation and type II inhibitors (quizartinib, sorafenib) which are inactive against most FLT3-TKD mutations, because they bind a region that is made inaccessible by TKD mutations (**Fig. 2**) (Muller and Schmidt-Arras 2020, Kennedy and Smith 2020, Ambinder and Levis 2021). Taken together, FLT3 meets all requirements to be a suitable target-antigen for the treatment of AML. Various therapeutic approaches targeting FLT3 have been developed and tested in the recent years, some of them will be discussed in the following.

1.4 T-cell-based immunotherapeutic strategies: CAR versus BiTE®

Recent technical advances offer the opportunity to overcome the issues related to TCR-based T-cell therapies by the generation of antibody-based antitumor receptors. The primary structure of the therefore utilized single chain fragment variables (scFvs) is based on variable regions derived from mAb. These scFvs are then specific for tumor antigens expressed both as MHC/peptide complexes and surface proteins (Maruta et al. 2019).

Chimeric Antigen Receptor (CAR) T cells

The strategy used in CAR-T cells is the expression of a recombinant chimeric antigen neo-receptor, consisting of an extracellular scFv, fused to the CD3ζ chain, which is an activating component of the TCR complex. First-generation CARs included only CD3ζ as intracellular signaling domain, second-generation CARs also include a single costimulatory domain derived from either CD28 or 4-1BB and third-generation CARs include two costimulatory molecules

(CD28, 4-1BB, or OX40) to promote proliferation and persistence. Fourth-generation CARs, also termed TRUCKs (T cells redirected for universal cytokine-mediated killing) have an enhanced antitumor activity due to additional genetic modification including transgenes for cytokine secretion (e.g., IL-12) or additional costimulatory ligands (Figure 3). When the target antigen is bound by the scFv, activating signals are triggered through the intracellular domains to mediate cytotoxic activity, cytokine production, proliferation, and survival. (Madduri et al. 2019, Aldoss et al. 2017, Subklewe et al. 2019).

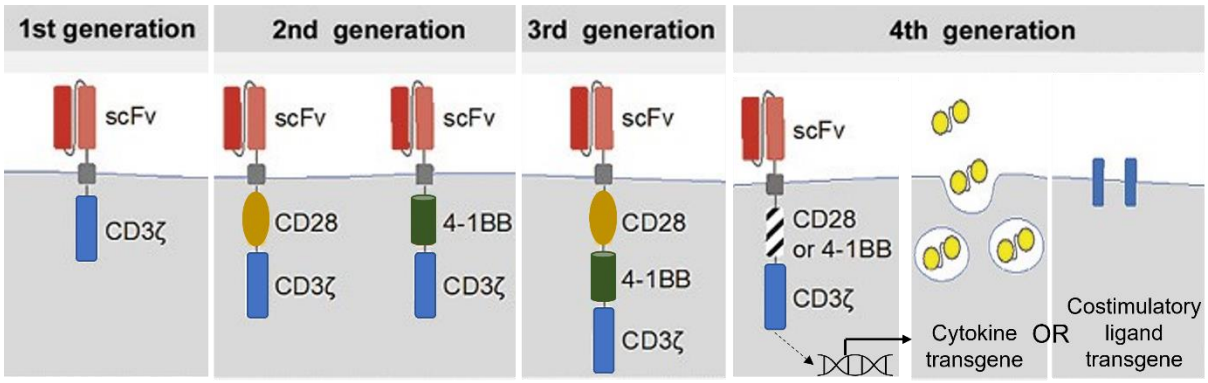

Figure 3: Evolution of CAR generations. First-generation CARs consist of a single chain fragment variable (scFv) and CD3ζ intracellular signaling domain. Second-generation CARs additionally include a single costimulatory domain (CD28 or 4-1BB), while third-generation CARs combine two costimulatory domains (e.g., CD28 and 4-1BB). Fourth-generation CARs harbor additional genetic modification, for example for cytokine secretion or additional costimulatory ligands. (Figure adapted from: Subklewe et al. (2019))

Various methods are utilized to introduce CARs into T cells, including *Sleeping Beauty* transposons, gamma retroviruses or HIV-derived lentiviral vectors. The goal is an efficient and stable gene transfer as well as transgene expression in T cells without facing the issues of gene silencing, mutagenesis, or subsequent development of T-cell lymphomas/leukemias as a consequence of DNA integration (Aldoss et al. 2017).

The production of CAR-T cells is comprised of several steps and is personalized for each patient. As a first step, PBMCs from the patient are collected by leukapheresis and transferred to a manufacturing facility. *Ex vivo* expansion of isolated $CD3^+$ or $CD4^+$ and $CD8^+$ T cells with anti-CD3, anti-CD28 mAb-conjugated beads or APCs like dendritic cells is carried out and the activated T cells are transduced with the designed vector coding for the CAR constructs. These genetically modified, tumor-reactive T cells are then expanded by coincubation with T-cell growth factors for 6 − 28 days. Finished CAR-T cells are washed and concentrated to a volume that can be infused into the patient after a lymphodepleting chemotherapy (Wang and Riviere

2016, Madduri et al. 2019) (**Fig. 4**). Two CAR-T cell products directed against CD19 were already approved by the FDA for the treatment of adult patients with relapsed or refractory large B-cell lymphoma (Slaney et al. 2018, Aldoss et al. 2017).

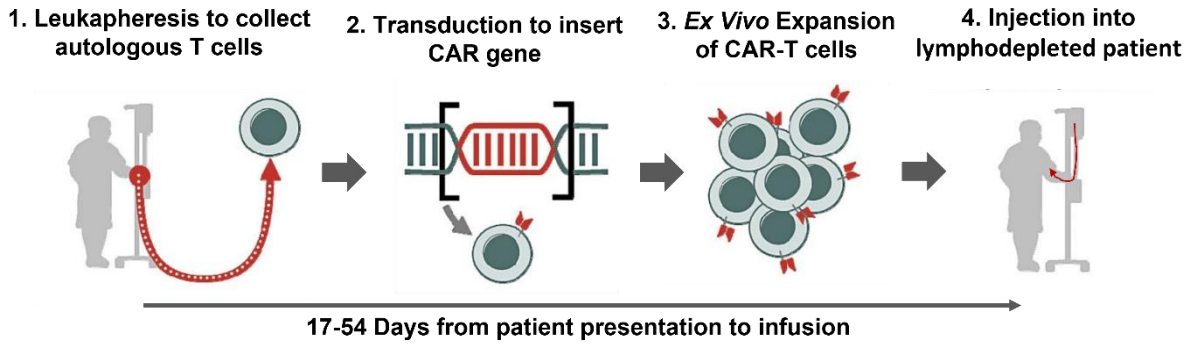

Figure 4: CAR-T cell treatment process. The clinical manufacturing of CAR-T cells starts with the isolation of patient T cells by leukapheresis. After an *ex vivo* expansion, T cells are transduced with the vector coding for the chimeric antigen receptor. Transduced T cells are further expanded, isolated, and administered by a single infusion to a lymphodepleted patient. (Figure adapted from: Subklewe et al. (2019))

Bispecific T-Cell Engagers (BiTEs®)

Another strategy to bypass the need of TCR/MHC interaction is the use of BiTE® constructs, which are recombinant bispecific proteins that have two scFvs from two different antibodies linked together by a short flexible linker. One scFv binds to a cell-surface molecule on T cells, typically the TCR complex protein CD3, and another one recognizes a target antigen expressed on the surface of malignant cells. By simultaneously binding to target antigens on tumor cells and the CD3 protein on T cells, BiTE® constructs induce the activation of T cells through the TCR signaling pathway and the formation of cytolytic synapses, leading to cytotoxic activity, and killing of tumor cells (Figure 5) (Slaney et al. 2018, Madduri et al. 2019). The first FDA approved BiTE® was Blinatumomab (Blincyto, Amgen) for relapsed B-cell precursor ALL, binding to CD19 on B cells and CD3ε. It is approximately one-third the size of a typical mAb, resulting in a rapid clearance and short serum half-life of approximately 2h. Therefore, a continuous intravenous infusion is needed to attain optimal steady-state concentrations and promote sustained T-cell activity. However, low picomolar concentrations are sufficient to achieve target cell lysis in both *in vitro* and *in vivo* (Aldoss et al. 2017, Madduri et al. 2019).

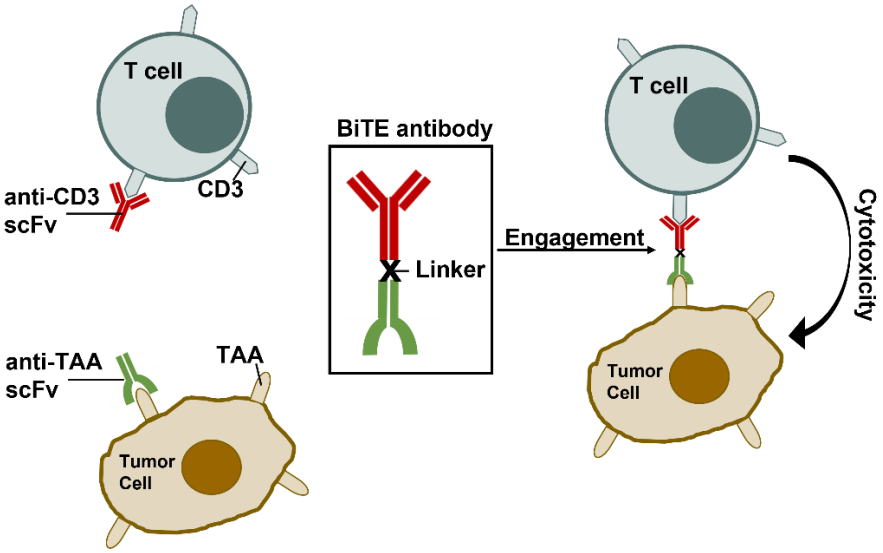

Figure 5: Bispecific T-cell Engager (BiTE®) technology. The BiTE® antibody consists of a scFv binding the T-cell receptor complex protein CD3 (red) and a scFv binding to a tumor associated antigen (TAA) (green) connected by a short flexible linker. Upon binding of the BiTE® antibody, T cell and tumor cell get in close proximity and T-cell activation is triggered, resulting in cytokine release and killing of the tumor cell. (Figure adapted from: Marayati et al. (2019))

T-cell types

T-cell populations predominantly consist of two subsets: cytotoxic CD8+ T cells whose primary function is the lysis of tumor cells and CD4+ helper T cells, which secrete cytokines to regulate immune responses. Based on differentiation states and functional abilities, T cells can be further classified into naïve T cells (T_N) and antigen-experienced or activated stem cell memory (T_{SCM}), central memory (T_{CM}), effector memory (T_{EM}), and effector (T_{EFF}) T cells (Slaney et al. 2018). For the manufacturing of CAR-T cells, cytotoxic and helper T-cell populations are mixed, with $CD8^+$ CAR-T cells rapidly clearing leukemic cells and thereby being the major cytotoxic players and $CD4^+$ CAR-T cells, which eradicated leukemia cells more slowly but were shown to have a longer persistence *in vivo* (Yang et al. 2015). Furthermore, it is now clear that CAR-T cells in a differentiated state have better efficacy *in vivo*, wherefor strategies favoring the generation and preservation of T_{SCM} and T_{CM} CAR-T cells are developed (Hurton et al. 2016). Similar to CAR-T cell therapy, also BiTE® constructs can activate both $CD8^+$ and $CD4^+$ T cells and again $CD8^+$ cells kill tumor cells faster than $CD4^+$ T cells. However, in contrast to CAR-T cell therapy, naïve T cells are not activated when engaged by BiTE® while antigen-experienced T-cell subsets mediate BiTE®-induced tumor cell lysis (Slaney et al. 2018). Large numbers of responding T cells and their continued action over prolonged time periods are

required to resolve malignant disease. By expansion *in vivo* and long-term engraftment following transfer, CAR-T cells meet these requirements. In some hematologic malignancies a more than 1,000-fold expansion of CAR-T cells was observed, and CAR-T cells in the blood made up more than 20 % of all circulating lymphocytes (Grupp et al. 2013, Porter et al. 2011). BiTEs® are less reliant on T-cell expansion, as substantial numbers of redirected T cells can be exploited from a large pool of antigen-experienced T cells already present in the patient. However, a 2- to 4-fold increase in circulating T cells has been described following BiTE® administration (Slaney et al. 2018).

T-Cell Synapse and Cytotoxicity

A central mechanism of action for lymphocytes to communicate via cell-cell interaction with APCs and antigen-specific target cells is the formation of an immune synapse (IS). The IS, also known as supramolecular activation cluster (SMAC) is comprised of three concentric rings. In the center (central SMAC; cSMAC), a concentration of TCRs and CD28 is found, wherefore the cSMAC is responsible for the key T-cell activation signaling events. The second ring (peripheral SMAC; pSMAC) is responsible for the stabilization of the cell-cell interaction and contains a series of adhesion molecules (including LFA-1/ICAM-1 interactions). The third ring (distal SMAC; dSMAC), is comprised of filamentous actin, that helps to exert a mechanical force on the synapse. Various forms of IS with special functions exist including the classical antigen recognition synapses, inhibitory synapses as well as cytolytic synapses (Strohl and Naso 2019). It was demonstrated that the structure and function of the BiTE® induced IS is highly similar to the normal cytolytic T-cell synapse. This similarity includes the formation of the three concentric rings and the presence of many proteins including LFA-1, LCK, CD3, CD2 and perforin (Offner et al. 2006). Synapses induced by CAR-T cells on the other hand were found to be significantly different from the classical T-cell synapse, as they are not highly organized as SMACs but rather disorganized, patchy signaling clusters lacking a defined structure. Further, CAR-T synapses do not form the characteristic pSMAC and do not require LFA-1 for stabilization (Davenport et al. 2018). These structural differences between BiTE® and CAR-T synapses also result in functional differences. A faster proximal signaling and recruitment of lysosomes to the IS can be observed for CAR-T cells, suggesting that they are able to mount a more rapid killing response than BiTEs®. Additionally, a significantly faster dissolution of the synapse and detachment from the target cell (off-rate) and a faster perforin and granzyme release were shown for CAR-T cells. In summary, CAR-T cells kill target cells faster and then also move on faster than BiTE®-activated T cells (Davenport et al. 2018, Strohl

and Naso 2019). Despite the differences in synapse formation, both BiTE®-engaged T cells and CAR-T cells can be subject to suppressing negative immunomodulation by immune checkpoints, wherefore clinical trials combining CAR-T cell or BiTE® treatment with checkpoint inhibition (e.g. anti-PD-1 and anti-CTLA4 antibodies) are running (Strohl and Naso 2019).

Toxicity and Adverse Effects

The most common toxicity that was observed with CAR-T cells therapy is the cytokine release syndrome (CRS), that occurs several hours to 14 days after CAR-T cell infusion. It is a systemic response due to large numbers of activated lymphocytes and/or myeloid cells that release inflammatory cytokines (e.g. IL-6 and IFNy) and is characterized by high fever, hypoxia, hypotension, fatigue, anorexia, tachycardia, capillary leak, and end-organ toxicity. CRS can be managed by anti-inflammatory treatment, including high-dose steroids and an anti-IL6 receptor antibody (tocilizumab) without inhibiting CAR-T cell treatment efficacy. Also, neurotoxicity termed as CAR-T cell–related encephalopathy syndrome (CRES) was reported, which is a toxic encephalopathic state characterized by symptoms of confusion, delirium, seizures, and cerebral edema. The pathophysiology of neurologic toxicity is not precisely known, but mechanisms are hypothesized to include cytokine-mediated endothelial activation and passive diffusion of cytokines into the central nervous system and/or trafficking of CAR-T cells into the cerebrospinal fluid. CRES can be managed by anti-inflammatory medication and seizure prophylaxis. Depletion of endogenous leukocytes by preconditioning regimens can also lead to cytopenia's (including neutropenia, anemia, and thrombocytopenia) as well as infections with microorganisms (Slaney et al. 2018, Madduri et al. 2019). As for CAR-T cell treatment, CRS is also the most frequent adverse effect upon BiTE® treatment, wherefor patients are required to be premedicated with dexamethasone, to reduce cytokine production. Also, a neurotoxic and metabolic encephalopathy-like syndrome is observed, with symptoms like headache, tremor, aphasia, and seizure. Other toxicities associated with BiTE® treatment are elevated liver enzymes, marrow suppression, infections, and electrolytes disturbances. However, short serum half-life of BiTE® allows for rapid dose adjustments in cases of severe adverse effects (Slaney et al. 2018, Aldoss et al. 2017, Madduri et al. 2019).

1.5 Aim and project outline

The aim of this thesis is to evaluate efficacy and function of experimental FLT3 CAR-T cells in comparison to an experimental FLT3 BiTE® antibody construct. The experimental FLT3 BiTE® consists of an anti-CD3 scFv and an anti-FLT3 scFv and was recently characterized by

Brauchle et al. (2020), demonstrating that it is capable of inducing T-cell dependent cellular cytotoxicity (TDCC) of FLT3-expressing cells *in vitro, in vivo,* and *ex vivo.*

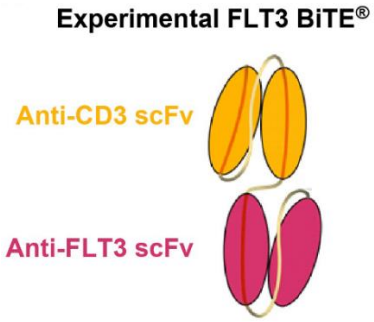

Figure 6: Cartoon depicting the experimental FLT3 BiTE® molecule. FLT3 BiTE® antibody comprise of a single chain fragment variable (scFv) binding the T-cell receptor complex protein CD3 (orange) and a scFv binding to the leukemia associated antigen FLT3 (magenta) connected by a short flexible linker. (Figure taken from: Brauchle et al. (2020))

Efficacy and function of both FLT3 CAR-T cells and BiTE® construct will be investigated *in vitro* using various FLT3 expressing or FLT3 negative human and murine cell lines (Ba/F3, MOLM-13, MV4-11, OCI-AML3, HEL 92.1.7), as well as *ex vivo* using primary human patient derived AML blasts from initial diagnose. The evaluation is based on flow cytometric analysis of simultaneous short or long term cocultures at various effector to target cell (E:T) ratios. Among others, antigen-specific cytotoxicity, degranulation (CD107a), T-cell exhaustion (PD-1, TIM3, LAG3) and immune synpase/conjugate formation should be examined. Further, the influence of CD86 costimulatory signal, checkpoint inhibitor co-therapy (anti-PD-1 antibody) and combination with FLT3 TKIs on FLT3 CAR-T cell and BiTE®-mediated cytotoxicity is of particular interest.

2 Material and Methods

2.1 Material

2.1.1 Biological material

After approval by the ethics committee of the Ludwig-Maximilians-Universität München (LMU, Munich, Germany) and a written informed consent in accordance with the Declaration of Helsinki, peripheral blood or bone marrow samples were collected from patients with AML at initial diagnosis as well as from healthy donors (HD). All samples were obtained from the Department of Medicine III, University Hospital, LMU Munich.

2.1.2 Cell lines

BA/F3

BA/F3 is an IL-3 dependent murine pro B cell line, whose precise origin is unclear as there is no paper describing the establishment of this cell line available. Evidence for a lymphatic background was provided by May-Gruenwald-Giemsa staining. Ba/F3 cell line has been used for a long time with the belief of a BALB/c origin, but a precise SNP analysis demonstrated that BA/F3 cell line was derived from a C3H mouse strain (DSMZ No: ACC 300). It is a model system for assessing both the potency and downstream signaling of kinase oncogenes (Warmuth et al. 2007). Ba/F3-FLT3^{WT} and Ba/F3-FLT3^{strong} cell line transduced to express human FLT3 were used in experiments, which were a kind gift by Prof. Dr. Spiekermann (Klinikum der Universität München, Munich).

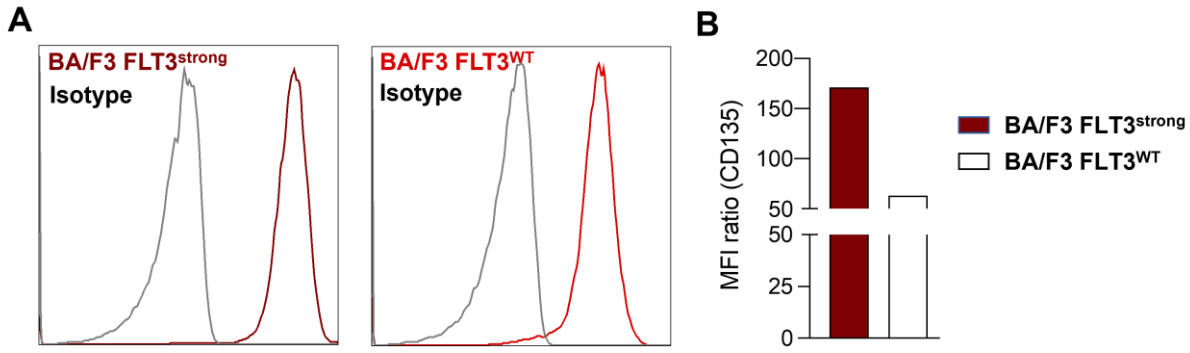

Figure 7. FLT3 surface expression on Ba/F3-FLT3^{WT} and Ba/F3-FLT3^{strong} cell line. A MFI of FLT3 (red) and isotype control (black). **B** *MFI ratio of FLT3 staining was calculated by dividing the MFI of CD135 by the isotype control.* BA/F3-FLT3^{strong} (red), BA/F3-FLT3^{WT} (white)

HEL 92.1.7

The human erythroleukemia (HEL) cell line was derived from a 30-year-old Caucasian man with Hodgkin's disease who later developed erythroleukemia (DSMZ No: ACC 11). Peripheral blood mononuclear cells from this patient at the time of relapse after an allogeneic bone marrow transplantation were used to initiate suspension cultures (Martin and Papayannopoulou 1982). As the HEL 92.1.7 cell line is FLT3 negative, it was used as a negative control for cytotoxicity experiments with FLT3 targeting CAR-T cells and the FLT3 BiTE® construct.

MOLM-13

The MOLM-13 cell line was established from the peripheral blood of a 20-year-old male patient at relapse of acute monocytic leukemia, FAB M5a, which had evolved from myelodysplastic syndrome (DSMZ No: ACC 554). It is an *in vitro* model for studying monocytic differentiation and leukemogenesis (Matsuo et al. 1997) and was used as FLT3-positive target cells in cytotoxicity experiments. MOLM-13 cells transduced to express PD-L1 (MOLM13+PD-L1) which were kindly provided by the AG Hopfner (Gene Center, LMU, Munich), where used to investigate the effect of immune checkpoint inhibitors on CAR-T cell and BiTE-engaged T-cell activity.

MS-5

The MS-5 cell line was established by irradiation of adherent cells in long-term bone marrow cultures derived from C3H/HeNSlc strain mice (DSMZ No: ACC 441). The cell line has the capacity to support the growth of hemopoietic stem cells for greater than 2 months *in vitro vitro* (Itoh et al. 1989). It was used to culture pAML blasts for up to 14 days.

MV4-11

MV4-11 cell line was generated from the blast cells of a 10-year-old male with biphenotypic B-myelomonocytic leukemia. It carries a translocation t(4;11) and a *FLT3*-ITD mutation (DSMZ No: ACC 102) (Lange et al. 1987). MV4-11 cells were used as FLT3-positive target cells in cytotoxicity experiments.

OCI-AML3

In 1987, the OCI-AML3 cell line was established from the peripheral blood of a 57-year-old man with acute myeloid leukemia (AML FAB M4) at diagnosis (DSMZ No: ACC 582). FLT3-positive OCI-AML3 cells were used to assess the antigen specific cytotoxicity of FLT3 CAR-T cells and FLT3 BiTE®.

Phoenix-ECO (P.Eco)

Phoenix is based on a human embryonic kidney line transformed with adenovirus E1a (293T cell line), which is carrying a temperature sensitive T antigen co-selected with neomycin. The cell line carries constructs, which are capable of producing ecotropic and amphotropic gag-pol and envelope virus protein. Therefore, it is a second-generation retrovirus producer cell line for the generation of helper-free ecotropic and amphotropic retroviruses (ATCC No.: CRL-3214™) (Nolan G., Stanford Cancer Institute).

Table 1: Cell line characteristics and culture conditions

Cell line	Organism	Cell Type /Tissue	Culture Properties	Culture media
BA/F3	*Mus musculus*, murine (mouse)	pro B cells	suspension	BA/F3 medium
HEL 92.1.7	*Homo sapiens*, human	Erythroleukemia (malignant blasts)	suspension	R10
K-562	*Homo sapiens*, human	chronic myeloid leukemia in blast crisis	suspension	R10
MOLM-13	*Homo sapiens*, human	acute myeloid leukemia	suspension	R10
MS-5	*Mus musculus*, murine (mouse)	stromal cells	adherent	Blast medium
MV4-11	*Homo sapiens*, human	biphenotypic B-myelomonocytic leukemia	suspension	R10
OCI-AML3	*Homo sapiens*, human	acute myeloid leukemia	suspension	R10
Phoenix-ECO	*Homo sapiens*, human	Kidney	adherent	P.Eco medium

2.1.3 Cell Culture Media

Table 2: Cell culture media

Medium	Components
BA/F3 Medium	500 ml RPMI 1640 10 % FBS 10 % WEHI cell line supernatant 1 % PSG
Blast Medium	500 ml Alpha MEM 12.5 % FBS 12.5 % Horse Serum 1 % PSG

P.Eco Medium	500 ml DMEM 10 % FBS 1 % PSG
R10	500 ml RPMI 1640 10 % FBS 1 % HEPES 1 % PSG
1x Cytokine Medium	Blast Medium rhu IL-3 rhu TPO rhu GCFS 57.4 µM ßME
Healthy donor Freezing Medium	90 % R10 10 % DMSO
Patient Freezing Medium	45 % RPMI 1640 45 % FBS 10 % DMSO

Table 3: Components for cell culture media

Name	**Catalogue Number**	**Manufacturer**
Alpha MEM	P04-21500	PAN-Biotec, DE
Dulbecco's Modified Eagle Medium (DMEM 1x)	42430-025	Thermo Fisher Scientific Inc., USA
Fetal Bovine Serum (FBS)	10270-106	Thermo Fisher Scientific Inc., USA
Hepes 1M Buffer Solution	15630-056	Thermo Fisher Scientific Inc., USA
Horse Serum	H1270	Merck KGaA, Germany
Penicillin-Streptomycin-Glutamine (100x, liquid) (PSG)	10378016	Thermo Fisher Scientific Inc., USA
rh G-CSF	300-23	PeproTech, Inc., USA
rh IL-3	200-03	PeproTech, Inc., USA
rh TPO	300-18	PeproTech, Inc., USA
RPMI 1640	P04-16500	PAN-Biotec, Germany
ß-Mercaptoethanol (ßME)	M3148	Sigma Aldrich, Germany

2.1.4 Antibodies

Table 4: Fluorophore-Conjugated Antibodies

Immunogen	Conjugate	Clone	Isotype	Catalogue number	Manufacturer
CD2 (human)	BV421	TS1/8	mIgG1,κ	309218	BioLegend, USA
	PerCP/Cy5.5	RPA-2.10	mIgG1,κ	300216	BioLegend, USA
CD3 (human)	BV421	UCHT1	mIgG1,κ	300434	BioLegend, USA
	APC	UCHT1	mIgG1,κ	300412	BioLegend, USA
CD4 (human)	FITC	OKT4	mIgG2b,κ	317408	BioLegend, USA
CD8 (human)	APC-Cy7	SK1	mIgG1,κ	344714	BioLegend, USA
CD11 (human)	FITC	Bu15	mIgG1,κ	337214	BioLegend, USA
CD14 (human)	FITC	61D3	mIgG1,κ	11-0149-42	Thermo Fisher Scientific Inc., USA
CD16 (human)	APC	3G8	mIgG1,κ	302012	BioLegend, USA
CD19 (human)	PE-Cy7	SJ25C1	mIgG1,κ	363012	BioLegend, USA
CD25 (human)	B421	BC96	mIgG1,κ	302630	BioLegend, USA
CD33 (human)	APC	WM53	mIgG1,κ	303408	BioLegend, USA
	PE-Cy7	WM53	mIgG1,κ	25-0338-42	Thermo Fisher Scientific Inc., USA
CD54 (ICAM) (human)	APC	REA266	mIgG1,κ	130-121-342	Miltenyi Biotec, DE
CD56 (human)	PerCP/Cy5.5	5.1H11	mIgG1,κ	362506	BioLegend, USA
CD69 (human)	APC	FN50	mIgG1,κ	310910	BioLegend, USA
CD86 (human)	APC	IT2.2	IgG2b	305412	BioLegend, USA
CD95 (FAS) (human)	PE	DX2	mIgG1,κ	305608	BioLegend, USA
CD107a (LAMP-1) (human)	FITC	H4A3	mIgG1,κ	328606	BioLegend, USA

CD135 (human)	PE	REA786	mIgG1,κ	130-111-587	Miltenyi Biotec, DE
	PE	SF1.340	mIgG1,κ	IM2234U	Beckman Coulter, USA
CD223 (LAG3) (human)	PE	11C3C65	mIgG1,κ	369306	BioLegend, USA
CD274 (PD-L1) (human)	BV421	MIH3	mIgG1,κ	374508	BioLegend, USA
	FITC	A17188B	mIgG2b, κ	621612	BioLegend, USA
CD279 (PD-1) (human)	PE-Cy7	EH12.2H7	mIgG1,κ	329918	BioLegend, USA
CD366 (TIM-3) (human)	BV421	F38-2E2	mIgG1,κ	345008	BioLegend, USA

Table 5: Isotype control antibodies

Isotype	**Conjugate**	**Clone**	**Catalogue number**	**Manufacturer**
IgG1, κ (mouse)	APC	MOPC-21	400120	BioLegend, USA
	APC	REA1017	130-117-099	Miltenyi Biotec, DE
	BV421	MOPC-21	400158	BioLegend, USA
	FITC	MOPC-21	400108	BioLegend, USA
	PE-Cy7	MOPC-21	400126	BioLegend, USA
	PE	MOPC-21	400112	BioLegend, USA
	PE	REA1017	130-117-098	Miltenyi Biotec, DE
	PE	679.1Mc7	A07796	Beckman Coulter, USA
IgG2b, κ (mouse)	FITC	MG2b-57	401206	BioLegend, USA

Table 6: Other Antibodies used in experiments

Name	**Specification**	**Catalogue number**	**Manufacturer**
Opdivo 10 mg/ml (Nivolumab)	40 mg/4 ml	PZN: 11024601	Bristol-Myers Squibb, UK
Purified anti-human CD11a/CD18 (LFA-1) Antibody	0.5 mg/ml	363402	BioLegend, USA
FLT3 BiTE®	500 µg/ml	-	Amgen, USA
Control BiTE® (cBiTE)	1620 µg/ml	-	Amgen, USA

2.1.5 Chemicals, Reagents and Buffers

Table 7: Chemicals and Reagents

Name	Catalogue Number	Manufacturer
0.5 M EDTA, pH 8.0	15575-038	Thermo Fisher Scientific Inc., USA
Calciumchlorid ($CaCl_2$)	21115	Merck, Germany
CellTrace CFSE	C34554 A	Thermo Fisher Scientific Inc., USA
CellTrace Far Red	C34564	Thermo Fisher Scientific Inc., USA
Dulbecco's Phosphate-Buffered Saline (DPBS)	P04-36500	PAN-Biotec, Germany
Dynabeads Human T-Activator CD3/CD28	11131D	Thermo Fisher Scientific Inc., USA
Formaldehyde	F1635	Merck, Germany
Gilteritinib	S7754	Selleckchem, USA
Histopaque-1077 Hybri-Max	H8889-500ML	Merck, Germany
LIVE/DEAD® Fixable Aqua Dead Cell Stain	L34966	Thermo Fisher Scientific Inc., USA
MACS BSA Stock Solution	130-091-376	Miltenyi Biotec, Germany
Heparin-Natrium-25000-ratiopharm	PZN: 03029843	Ratiopharm, Germany
Polybrene Transfection Reagent	TR-1003-G	Merck, Germany
Quizartinib	S1526	Selleckchem, USA
Sorafenib	S7397	Selleckchem, USA
T cell TransAct™	130-111-160	Miltenyi Biotec, Germany
Trypan Blue Stain (0.4 %)	T10282	Thermo Fisher Scientific Inc., USA
Trypsin EDTA 0,05 %	25300054	Thermo Fisher Scientific Inc., USA

Table 8: Buffers

FACS Buffer	500 ml PBS 0.2 % BSA (stock: 20 %) 2 mM EDTA (stock: 0.5M)
FACS Fix	50 ml FACS Buffer 2 % Formaldehyde (37 %)

2.1.6 Kits

Table 9: Kits for cell isolation

Name	Cat. Number	Manufacturer
EasySep™ Human T Cell Isolation Kit	#17951	Stemcell Technologies, USA
EasySep™ Human CD3 Positive Selection Kit II	#17851	Stemcell Technologies, USA

2.1.7 Equipment

Table 10: Equipment used in experiments

Name	Catalogue Number	Manufacturer
CO_2 incubator	CB 150	BINDER GmbH, Germany
Countess II automated cell counter	A27978	Thermo Fisher Scientific Inc., USA
CytoFLEX S Flow Cytometer	-	Beckman Coulter, USA
Inverted Laboratory Microscope	DM IL	Leica Microsystems GmbH, Germany
MoFlo Astrios EQ Cell Sorter	-	Beckman Coulter, USA
Mr. Frosty™ Freezing Container	5100-0001	Thermo Fisher Scientific Inc., USA
Rotina 420R	4706	Andreas Hettich GmbH & Co. KG, Germany
Safety Cabinet, Class II	51027621	Thermo Fisher Scientific Inc., USA
Sprout Mini Centrifuge	120395	Heathrow Scientific, USA
Water bath VWB 12	462-0242	VWR International GmbH, Germany

2.1.8 Consumables

Table 11: Consumables used in experiments

Name	Catalogue Number	Manufacturer
15 ml conical tube	352096	Corning Incorporated, USA
25 ml Reagent Reservoir	613-1175	VWR International GmbH, Germany
3 ml Syringe	30958	BD Switzerland Sarl, CH
5 ml round-bottom tube	352235	Corning Incorporated, USA
50 ml centrifuge tube	430829	Corning Incorporated, USA
50 ml Syringe	8728844F-06	B. Braun SE, Germany
6 Well tissue culture plate	353224	Corning Incorporated, USA
96 Well tissue culture plate	353077	Corning Incorporated, USA
Cell Culture Dish	0030 702.018	Eppendorf AG, Germany
Countess cell counting chamber slides	C10283	Thermo Fisher Scientific Inc., USA
Cryogenic Vials 1 ml	123263	Greiner Bio-One International GmbH, AT
Cryogenic Vials 1,8 ml	E3110-6122	STARLAB, UK
Graduated TipOne® Tip 10, 100, 1000 µl	S1110-3700	STARLAB, UK
Injekt-F	9166017V	B. Braun SE, Germany
Microlance	301500	BD Switzerland Sarl, CH

Pasteur pipette	612-1747	VWR International GmbH, Germany
PCR SingleCap 8er-SoftStrips 0.2 ml	710984	Biozym Scientific GmbH, Germany
Serological pipette 5, 10, 20 ml		Corning Incorporated, USA
Syringe filters (0,22 µm)	P666.1	Carl Roth GmbH + Co. KG, Germany
T25 cell culture flask	FALC353108	Omnilab-Laborzentrum GmbH & Co. KG, Germany
T75 cell culture flask	FALC353136	Omnilab-Laborzentrum GmbH & Co. KG, Germany

2.2 Methods

2.2.1 Cell culture: Maintenance of cell lines

Cell lines were cultured at 37 °C and 5 % CO_2 (CO_2 incubator, BINDER GmbH, DE) in the respective culture medium specified in Table 1. BA/F3, HEL 92.1.7, K-562, MOLM-13, MV4-11 and OCI-AML3 were split every 2-3 days.

To split the adherent P.Eco and MS-5 cell lines, medium was removed, adherent cells were washed once with sterile DPBS (Dulbecco's Phosphate-Buffered Saline, PAN-Biotec, Germany) and dissolved with Trypsin (Trypsin EDTA 0,05 %, Thermo Fisher Scientific Inc., USA). After 2-3 min of incubation, the reaction was stopped by adding prewarmed culture medium. The Phoenix-ECO cells were washed once for 5 min at 550 rcf (Rotina 420R, Andreas Hettich GmbH & Co. KG, DE) and resuspended before splitting, for the MS-5 this was omitted in order not to clump them together. Both cell lines were split every 3 days.

2.2.2 Isolation of human peripheral blood mononuclear cells (PBMCs) from whole blood

Before drawing blood, 50 ml syringes (B. Braun SE, Germany) were coated with Natrium-Heparin (Heparin-Natrium-25000-ratiopharm, Ratiopharm, Germany) and a maximum of 300 ml peripheral blood was drawn from HD donors. Whole blood was then diluted 1:1 with sterile DPBS. 15 ml Ficoll-Paque (Histopaque-1077 Hybri-Max, Merck, Germany) was placed at the bottom of a 50 ml conical tube and ~35 ml diluted blood was slowly layered over the Ficoll-Paque. The tube was centrifuged for 30 min at 820 rcf without brake and afterwards the buffy coat containing the PBMCs was carefully isolated with a Pasteur pipet (VWR International GmbH, DE). The isolated PBMC's were washed in sterile DPBS for 10 min at 550 rcf with brake and the cell pellet was resuspended with sterile DPBS again for counting. An aliquot of the cell suspension was taken, mixed 1:1 with Trypan Blue (0.4 %, Thermo Fisher Scientific Inc., USA) and the cell count was determined with a Countess (II) automated cell counter (Thermo Fisher Scientific Inc., USA). The isolation of bone marrow mononuclear cells (BMMCs) out of bone marrow sample received form the LMU hospital was carried out according to the same protocol, but the bone marrow was diluted 1:3 with DPBS before layering on the Ficoll-Paque.

For the isolation of T cells from PBMC's, the EasySep™ Human T Cell Isolation Kit (STEMCELL Technologies, USA) was used according to the manufacturer's instructions.

CAR-T cell production

Isolated T cells were activated with T Cell TransACT™ (Miltenyi Biotec, Germany) for 24h before viral transduction at 800 rcf for 30 min. The transduced T cells were rested for 48h at 37 °C and 5 % CO_2 before further culture.

2.2.3 Cryopreservation

Cell lines, isolated PBMCs or T cells were centrifuged for 5 min at 550 rcf and a concentration of 5 x 10^6 to 5 x 10^7 cells/ml were slowly resuspended in 1,5 ml cold cell culture freezing medium per cryotube. The cryotubes were immediately transferred into a freezing container (Mr. Frosty™, Thermo Fisher Scientific Inc., USA), to enable a step wise cooling rate of 1 °C/min and put in a -80 °C freezer. The samples were transferred to the -150 °C freezer or to liquid nitrogen after 1-2 days.

2.2.4 Thawing of cells

Frozen cryotubes containing cell lines, T cells, PBMCs or BMMCs were placed into a 37 °C water bath (Water bath VWB 12, VWR, DE) to thaw. The cell suspension was transferred into 15 ml tubes and HD or cell line samples were diluted with the respective prewarmed culture medium, patients samples were diluted with cold FACS Buffer. The cells were centrifuged at 550 rcf for 5 min, and the cell pellet was resuspended in prewarmed complete culture medium. PBMCs, BMMCs and T cells were then ready to use for assays. Cell lines were transferred to a T25 or T75 cell culture flask (Omnilab-Laborzentrum GmbH & Co. KG, DE) to culture them under the respective conditions.

2.2.5 Antibody staining for flow cytometric analysis

96-well-plates containing the cells were centrifuged for 5 min at 550 rcf, the supernatants were discarded, and the cells were washed in 200 µl FACS buffer again for 5 min at 550 rcf. The cell pellet was then resuspended in 20 µl FACS buffer. Staining antibodies for surface markers of interest and a cell viability dye (LIVE/DEAD® Fixable Aqua Dead Cell Stain, Thermo Fisher Scientific Inc., USA) were added in an amount determined by titration. The cells were incubated for 20-30 min at 4 °C protected from light. The cells were then washed with 200 µl FACS buffer for 5 min at 550 rcf and then resuspended in 200 µl FACS buffer if analyzed directly. For a later measurement timepoint, stained cells were fixed in 200 µl FACS Fix and placed in at 4 °C until usage. Measurement was carried out with a CytoFLEX S Flow Cytometer (Beckman Coulter, USA) and analyzed with FlowJo Software (Version 10.7.1, Becton Dickinson GmbH, Germany)

The strength of surface expression of a protein of interest was determined by the mean fluorescence intensity (MFI) ratio, which was calculated as follows. In our laboratory, a threshold of an MFI ratio > 1.5 was set for measurable surface expression.

$$\text{MFI ratio} = \frac{\text{MFI Target Antigen}}{\text{MFI Isotype}}$$

2.2.6 FLT3 surface expression on mature hematopoietic cells

To determine the FLT3 surface expression, the cells were stained with two staining panels both containing CD135-PE (clone: SF1.340, Beckman Coulter, USA) or mIgG1κ-PE isotype (clone: 679.1Mc7, Beckman Coulter, USA) and a viability dye. Panel 1 included CD3-BV421 (clone: UCHT1, BioLegend, USA) for T cells, CD56-PC5.5 (clone: 5.1H11, BioLegend, USA) for NK cells and CD14-FITC (clone: 61D3, Thermo Fisher Scientific Inc., USA) for monocytes. Panel 2 included CD19-PC7 (clone: SJ25C1, BioLegend, USA) for B cells and CD11c-FITC (clone: Bu15 BioLegend, USA) for DCs.

2.2.7 Transfection of P.Eco cells

5×10^6 P.Eco cells were seeded in 10 ml P.Eco Medium in a culture plate and incubated overnight at 37 °C and 5 % CO_2. The day after the old medium was exchanged, and the plate was incubated for 4 h at 37 °C, 5 % CO_2. For the transfection, one sterile round-bottom tube was prepared with 13 µg of the respective DNA, filled up to 450 µl with H_2O and 50 µl $CaCl_2$ (Merck, Germany) was added. A second tube was prepared with 500 µl Hepes Buffer Solution (Thermo Fisher Scientific Inc., USA). The content of tube one was then added to tube two in a dropwise manner, mixed and incubated for 3-4 min at room temperature. The mixture was then added to the P.Eco culture plate in a dropwise fashion, was equally distributed and the plate was incubated overnight at 37 °C and 5 % CO_2. The next day the media was refreshed, and the plate was incubated overnight at 37 °C, 5 % CO_2 again. On day four, the viral supernatant was taken off, filtered two times with a 40 µm filter (Rotilabo-syringe filters, Carl Roth GmbH + Co. KG, Germany) and put in a -80 °C freezer if not used directly.

2.2.8 Transduction of BA/F3 cells

$1{,}5 \times 10^6$ BA/F3 cells were resuspended in 3 ml BA/F3 medium, 4,8 µl Polybrene transduction reagent (Merck, Germany) was added to the tube and mixed by vortexing. 3 ml viral supernatant were added, and the content of the tube was equally separated into two wells of a 6-Well plate. The plate was centrifuged in a preheated centrifuge for 90 min at 1565 rcf at 30 °C and afterwards incubated for 2,5 h at 37 °C and 5 % CO_2. After incubation, 2 ml fresh

BA/F3 medium was added to each well and the cells were incubated for two days at 37 °C, 5 % CO_2. The transduction efficiency was then assessed via flow cytometry by staining the cells for the transduced surface marker. If the transduction was successful, the cells were sorted with a cell sorter (MoFlo Astrios EQ Cell Sorter, Beckman Coulter, USA) to get 2 x 10^6 cells positive for the transduced antigen. The sorted cells were incubated in a T25 cell culture flask for 4 days at 37 °C, 5 % CO_2 and after two days the medium was refreshed. 200 µl aliquots were then taken from the cell suspension and again stained for the transduced surface marker to see if the sorting was successful. If so, cells were transferred in a T75 cell culture flask with fresh medium. Six days after the first sort, the cells were again sorted to get 2 x 10^6 cells with a high purity and were further cultured under normal BA/F3 conditions until usage.

2.2.9 TDCC Assay

FLT3 CAR-T cells or HD T cells were cocultured with target cells at an E:T ratio of 1:3, 1:5 and 1:10. 5 ng/ml FLT3 BiTE® was added to the wells with the HD T cells. Untransduced (UT) T cells or 5 ng/ml control BiTE® (cBiTE) were used as negative controls. The cells were incubated for 3-6 days at 37 °C, 5 % CO_2 before antibody staining and flow cytometric analysis. Cytotoxicity was determined based on the specific lysis and calculated as follows:

$$\% \text{ Specific Lysis} = \left(1 - \frac{\text{target cell count FLT3 CAR-T cells or BiTE®}}{\text{target cell count UT-T cells or cBiTE®}}\right) * 100$$

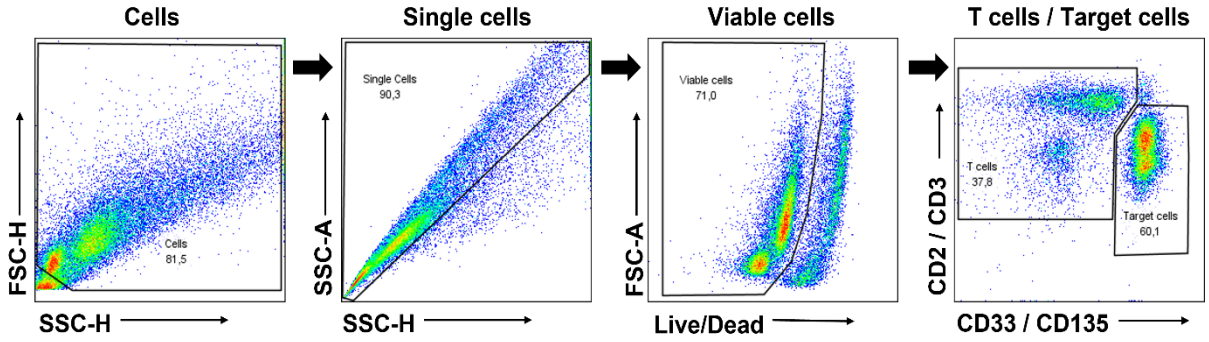

Figure 8: Gating strategy for TDCC assays. T cells and target cells were identified and discriminated from debris by size and granularity using FSC/SSC. Doublets were excluded by SSC-A/SSC-H and viable cells were identified by Live/Dead marker. Among viable cells, $CD2^+/CD3^+$ T cells were separated form $CD33^+/CD135^+$ target cells, depending on the assay set up.

2.2.10 CD107a degranulation Assay

A total number of 4×10^5 cells per well were seeded at an E:T ratio of 1:10, BA/F3-FLT3^{stong}CD86 were used as target cells. 5 ng/ml BiTE®/cBiTE® were added to the appropriate wells. The cells were cocultured in presence of 1 µg CD107a-FITC antibody (clone: H4A3, BioLegend, USA) or mIgG1κ-FITC isotype (clone: MOPC-21, BioLegend, USA) for up to 48 h at 37 °C, 5 % CO_2. For the 24 h and 48 h read out, additional 1 µg CD107a-FITC antibody or mIgG1κ-FITC isotype were added to the appropriate wells 30 min before staining. To analyze CD107a degranulation, cells were stained for CD3-BV421 (clone: UCHT1, BioLegend, USA), CD135-PE (Miltenyi Biotec, DE) and viability after 2, 4, 24 and 48 h and CD107a MFI ratio was calculated for CD3$^+$ cells.

2.2.11 Conjugate formation Assay

BA/F3-FLT3^{stong}CD86 were stained with CFSE (CellTrace CFSE, Thermo Fisher Scientific Inc., USA) and T cells were stained with Far Red (CellTrace Far Red, Thermo Fisher Scientific Inc., USA) according to the manufacturer's instructions. Half of the T cells were incubated with 20 µg/mL of a purified anti-human LFA-1 antibody (clone: m24, BioLegend, USA) at 37 °C, 5 % CO_2 for 30 min. Stained cells were cocultured at an E:T ratio of 1:1 with a total amount of 1×10^6 cells per well under following conditions: CAR-T, T cells+ BiTE®, UT T cells + BiTE®, T cells, UT T cells with or without LFA-block. At the start of the experiment, cells were spun down for 1 min at 300 rcf, carefully mixed by pipetting up and down (2-3x) and then incubated for up to 2 h at 37 °C, 5 % CO_2. After 10, 30, 60, 120 and 240 min, the reaction was stopped by adding 100 µl prewarmed FACS Fix. The cells were fixed for 15 min at 37 °C, washed once for 1 min at 300 rcf and were carefully resuspended in 200 µl FACS Fix for analysis. Conjugate formation of T cells with target cells was assessed by the percentage of the CFSE$^+$FarRed$^+$ double positive population and normalized to all FarRed$^+$ T cells.

2.2.12 PD-1 blocking Assay

T cells were stained with FarRed as previously described and cocultured MOLM13+PD-L1 at E:T ratios of 1:3, 1:5 and 1:10. 5 ng/ml BiTE® or cBiTE® were added to the appropriate wells and 10 µg/ml PD-1 blocking antibody (Opdivo 10 mg/ml (Nivolumab), Bristol-Myers Squibb, UK) were added, whereas controls were left untreated. Plates were incubated for 3-6 days at 37 °C, 5 % CO_2. Every 3 days, half of the medium was exchanged. On day 0, 3 and 6, cells were stained with CD33-PC7 (clone: WM53, Thermo Fisher Scientific Inc., USA), PD-1-FITC

(clone: A17188B, BioLegend, USA) or mIgG2b,κ-FITC isotype (clone: MG2b-57, BioLegend, USA) and viability for flow cytometric analysis.

2.2.13 Modulating the Activity of FLT3 CAR-T cells or FLT3 BiTE® through Tyrosine Kinase Inhibitors

T cells were cocultured with either MOLM-13 or MV4-11 cells at E:T ratios of 1:5, 1:10 and 1:20 in 200 µl R10 medium. 5 ng/ml BiTE® or cBiTE® were added to the appropriate wells. In addition, the TKI Quizartinib (Selleckchem, USA) was added at concentrations of 1 nM and 50 nM, Sorafenib (Selleckchem, USA) at 40 nM and 400 nM and Gilteritinib (Selleckchem, USA) at 1 nM and 80 nM, whereas controls were left untreated. Conditions with only MOLM-13, MV4-11 or T cells stimulated with CD3xCD28 beads (Dynabeads Human T-Activator CD3/CD28, Thermo Fisher Scientific Inc., USA) treated or untreated with the TKIs were integrated as additional controls to assess the effect of the TKIs especially on target or effector cells. The cocultures were incubated for 72 h at 37 °C and 5 % CO_2 before analysis by flow cytometry. Cells were stained for CD33-APC (clone: WM53, BioLegend, USA), CD2-BV421 (clone: TS1/8, BioLegend, USA), CD135-PE (clone: SF1.340, Beckman Coulter, USA) or mIgG1κ-PE (clone: 679.1Mc7, Beckman Coulter, USA) and viability.

2.2.14 Bystander Killing Assay

The FLT3 expressing cell line MOLM-13 was stained with CFSE and the FLT3 negative cell line HEL 92.1.7, which served as bystander cell line, was stained with FarRed as previously described. T cells, $FLT3^+$ target cells and $FLT3^-$ bystander cells were cocultured in an E:T ratio of 1:3 with a total cell number of 200.000 cells/well at different percentages of bystander cells, indicated in Table 12. The cocultures were incubated for 72 h at 37 °C and 5 % CO_2. For flow cytometric analysis, cells were stained for CD2-BV421 (clone: TS1/8, BioLegend, USA), CD54-APC (clone: REA266, Miltenyi Biotec, DE), CD95-PE (clone: DX2, BioLegend, USA) and viability.

Table 12: Percentage of bystander cells with corresponding volume of HEL 92.1.7 and MOLM-13 cells per well

Percentage of bystander cells	Volume of HEL 92.1.7 (bystander) per well	Volume of MOLM-13 (target) per well
100 %	100 µl	0 µl
75 %	75 µl	25 µl
50 %	50 µl	50 µl
25 %	25 µl	75 µl
0 %	0 µl	100 µl

2.2.15 Mimicking Continuous Stimulation of T cells *in vitro*

T-cell long-term co-cultures were carried out according to Zieger et al. (2020). HD T cells with FLT3 BiTE® or FLT3 CAR-T cells were cocultured in the presence of BA/F3-FLT3^{stong}CD86 cells for 28 days. Between day 7 and 28, T cells were harvested from the coculture every 3-4 days. CAR- and BiTE®-mediated cytotoxicity of the harvested T cells was assessed in context of a TDCC assay with BA/F3-FLT3^{stong}CD86 as target cells and the proliferative capacity during the cytotoxicity assay was evaluated by calculating fold change of $CD2^+$ counts. The cells were stained for CD2-BV421, CD135-PE (Beckman Coulter) and PD-1-FITC.

2.2.16 TDCC Assay with HD bone marrow

2 x 10^5 HD BMMCs per well were cocultured at E:T ratios of 1:3, 1:5 and 1:10 in Blast Medium. For the BiTE® condition, 5 ng/ml FLT3 BiTE® or cBiTE® were added to the respective well. The cocultures were incubated for 72 h at 37 °C, 5 % CO_2, cells were stained for CD2-BV421 and CD135-PE or mIgG1κ-PE (Beckman Coulter) and analyzed by flow cytometry.

2.2.17 TDCC Assay with primary AML blasts

Ex vivo long-term culture of pAML blasts was carried out as previously described (Krupka et al. 2014). Before usage of the pAMLs, T cells were depleted from the pAML blasts with a EasySep™ Human CD3 Positive Selection Kit II (Stemcell Technologies, USA) according to the manufacturer's manual to achieve exact E:T ratios. pAML blasts and T cells were cocultured in 200 µl 1x Cytokine Medium on MS-5 feeder cells at variating E:T ratios. 5 ng/ml BiTE® or cBiTE® were added to the appropriate wells. The cocultures were incubated at 37 °C, 5 % CO_2 for 3-14 days. Every three days, half of the old medium was exchanged. The cells were stained for CD2-BV421, CD135-PE or mIgG1κ-PE (Beckman Coulter), CD33-APC (clone: WM53, BioLegend, USA) and PD-1-FITC or mIgG2b,κ-FITC.

2.2.18 Statistical analysis

Statistical analysis was performed using Prism software (v9.0.0, GraphPad, USA). Unpaired Student's t-tests were used to determine the significance of the differences between groups in *in vitro* experiments. A significant difference was accepted when P-values < 0.05. All graphs reported as mean ± SEM values of at least three biological replicates unless otherwise stated. Values given in the text are the arithmetic means of all replicates.

3 Results

3.1 FLT3 surface expression on mature hematopoietic cells

The MFI ratio of all examined mature hematopoietic cells isolated from HD blood was >1.5, indicating that the cells were positive for FLT3 surface expression. However, only a low FLT3 expression slightly above the threshold was observed for most cell types **(Fig. 9A)**. Further, all cell types were analyzed for the proportion of FLT3$^+$ in the whole subpopulation given in percentage. A portion of cells were FLT3$^+$ within each examined subpopulation. The highest percentage of FLT3$^+$ cells was found in the monocyte subpopulation (Ø 27 %), followed by dendritic cells (Ø 18 %) and NK cells (Ø 16 %). B cell (Ø 8.8 %) and T cell (Ø 4.7 %) populations only had a low proportion of FLT3$^+$ cells **(Fig. 9B)**. In summary, all examined cell types only had a low proportion of FLT3$^+$ cells and these positive cells had only a low level of expression, indicated by low MFI ratios. It can therefore be concluded that mature hematopoietic cells are unlikely to be attacked by FLT3-directed T cells.

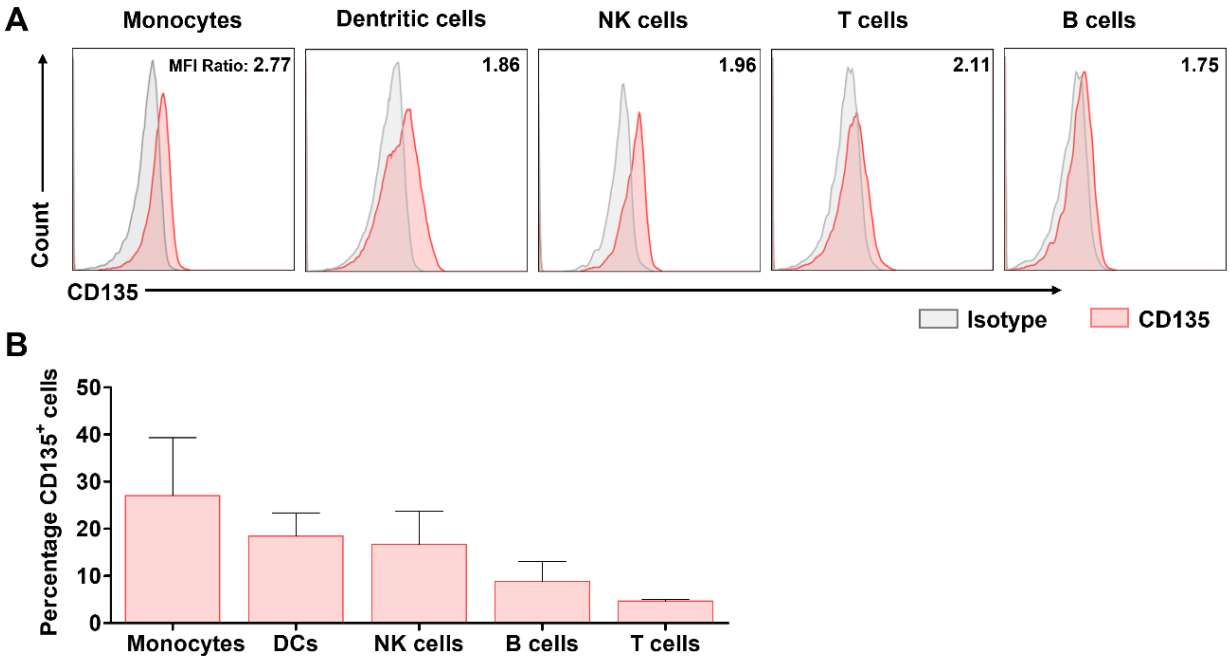

Figure 9: FLT3 surface expression on mature hematopoietic cells. A Overlays of anti-CD135 signals of dendritic cells, monocytes, B cells, T cells and NK cells derived from HD PBMCs determined by flow cytometry. CD135 MFI ratios were calculated by dividing the MFI of CD135 mAb (red) by the isotype control (grey). Given values are the arithmetic mean of 3 replicates**. B** Proportion of CD135$^+$ cells in percentage (%). Error bars represent mean +/- SEM. n=3.

3.2 FLT3 CAR-T and BiTE® construct mediate antigen-specific cytotoxicity against FLT3$^+$ leukemic cell lines

To evaluate the specific cytotoxicity of FLT3 CAR-T cells and the FLT3 BiTE® construct against AML cells, FLT3 expression on various AML cell lines was analyzed by flow cytometry and MFI ratio as well as proportion of FLT3$^+$ cells were calculated. The FLT3 expressing leukemic cell lines OCI-AML3 (MFI ratio: Ø 6.38, %FLT3$^+$ cells: Ø 81.9), MOLM-13 (MFI ratio: Ø 3.92, %FLT3$^+$ cells: Ø 69.5) and MV4-11 (MFI ratio: Ø 1.67, %FLT3$^+$ cells: Ø 17.3) were used as target cells (**Fig. 10A**). The cell line HEL 92.1.7 (MFI ratio: Ø 1.36, %FLT3$^+$ cells: Ø 3.59) was used as FLT3-negative (FLT3$^-$) control target cell line as previously described (Brauchle et al. 2020). UT-T cells and cBiTE® were used as control constructs. Primary data already indicate dying of FLT3$^+$ target cells, as decreasing target cell populations are observed in cocultures with MV4-11, MOLM-13 and OCI-AML3 (**Fig. 10B**). As shown in **Fig. 10C**, over 40 % of MOLM13, MV4-11 and OCI-AML3 cells were lysed by both FLT3 CAR-T cells and BiTE®-engaged T cells after 3 days at the lowest E:T ratio of 1:10. The specific lysis increased with a higher proportion of T cells in the coculture, so that a specific lysis of up to 80 % was reached at an E:T ratio of 1:3 after 3 days. The lysis mediated by the FLT3 BiTE® treatment was overall slightly higher than with CAR treatment. After 6 days, over 80 % of MOLM13, MV4-11 and OCI-AML3 cells were killed with both FLT3 CAR-T cell and BiTE® treatment. Even if the MFI ratios and the proportion of FLT3$^+$ cells varied a lot between the different cell lines, the observed lysis was comparable for all of them after 3 and 6 days. To determine if the observed lysis of FLT3$^+$ cell lines was indeed FLT3-specific, lysis of FLT3$^-$ HEL 92.1.7 cells was examined. FLT3 CAR-T cells mediated no lysis of FLT3$^-$ HEL 92.1.7 cells. After 3 days, also no lysis of HEL 92.1.7 cells was recognized upon FLT3 BiTE® treatment. However, after 6 days, the BiTE® constructed mediated a low lysis (>10 %) of FLT3$^-$ cells at the E:T ratios 1:3 and 1:5 (**Fig. 10C**).

These results generally indicate that the level of FLT3 surface expression on FLT3$^+$ target cells does not appear to directly correlate with the level of target cell lysis and the influence of other factors, such as mutation status, may need to be considered. Overall, both FLT3 CAR and BiTE® construct mediated a potent specific lysis of FLT3$^+$ target cells. Treatment with FLT3 BiTE® tended towards a slightly higher lysis of FLT3$^+$ target cells than with FLT3 CAR-T cells. On the other hand, the FLT3 BiTE® construct also mediated a low unspecific lysis of FLT3$^-$ cells while the HEL 92.1.7 cells tended to grow out upon treatment with FLT3 CAR-T cells.

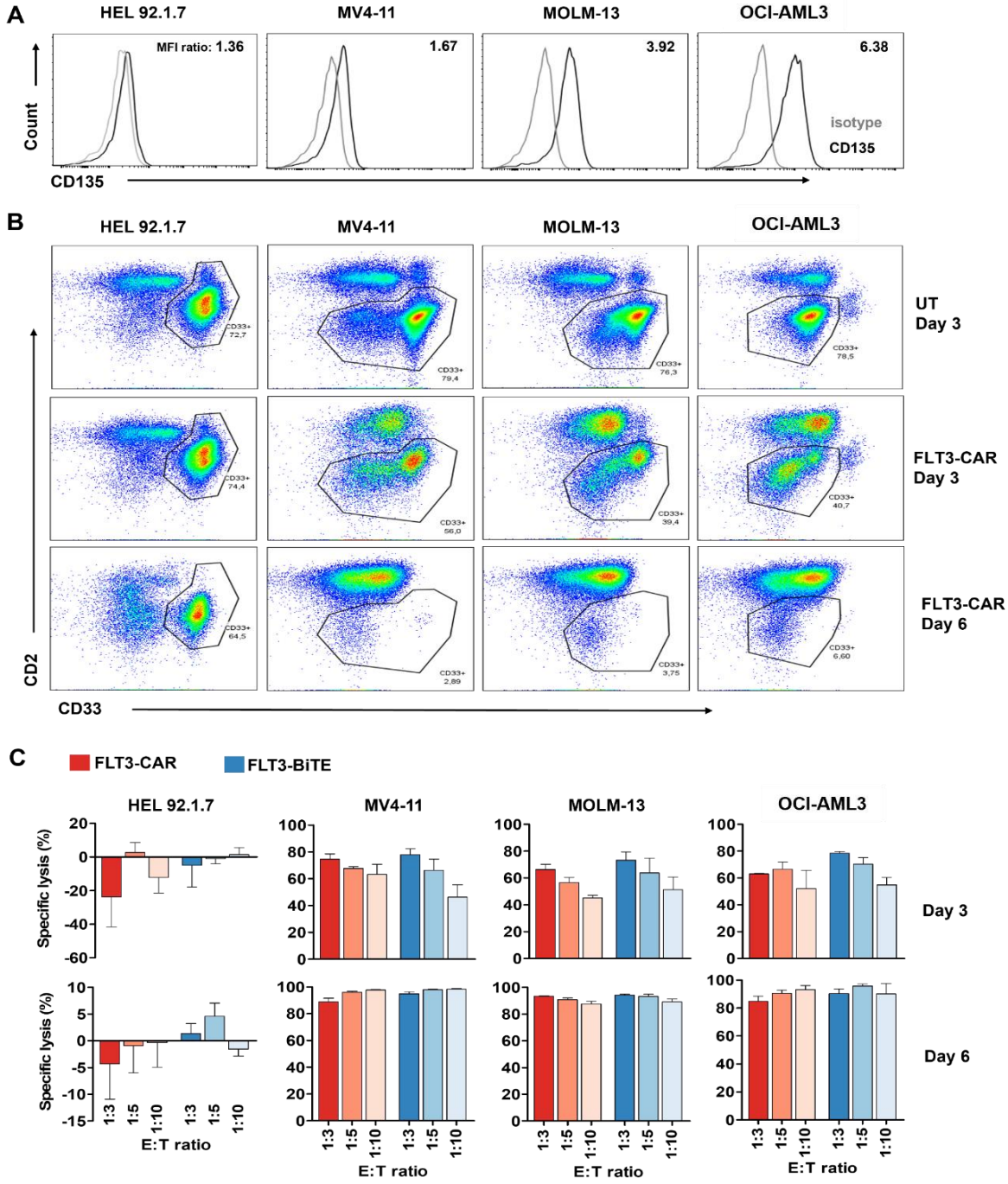

Figure 10: FLT3 CAR-T and BiTE® construct mediate antigen-specific cytotoxicity against FLT3⁺ cell lines.
A FLT3 surface expression on leukemic cells lines HEL 92.1.7, MV4-11, MOLM-13 and OCI-AML3 were analyzed by flow cytometry. MFI ratio of the FLT3 staining was calculated by dividing the MFI of anti-CD135 (black) by the MFI of the isotype control (grey) and a MFI>1.5 was set as threshold for FLT3-positive cells. Given values are the mean of 3 replicates. **B** Percentage of CD33⁺ target cells after co-culture with CAR-T or control UT-T cells at an E:T ratio of 1:3 for 3 or 6 days determined by flow cytometry. **C** Lysis of FLT3⁺ or FLT3⁻ leukemic cell lines mediated by FLT3 CAR-T and BiTE® construct. Target and effector cells were co-cultured for 3 or 6 days at the indicated E:T ratio. BiTE® concentration: 5 ng/ml. Error bars represent mean +/- SEM. n=3.

3.3 Conjugate formation

The level of stable immune synapses, formed by FLT3 CAR or TCR/FLT3 BiTE® interactions and the role of LFA-1 binding to its ligand (ICAM-1) on tumor cells in forming these stable synapses was assessed by a flow cytometry-based conjugate assay (**Fig. 11A**). Conjugate formation of FLT3 CAR-T cells with BA/F3-FLT3^{stong}CD86 target cells was at a stable level of ~27 % of total CAR-T cells in conjugates with targets between 10 to 60 min of coculture (**Fig. 11B**). Thereafter until 240 min a slight decrease in the proportion of conjugate-forming CAR-T cells was observed (240 min: Ø 21.2 %). With LFA-1 blocking, the percentage of CAR-T cells in conjugates was at the same level as without blocking after 10 min of coculture but was then slightly lower for each additional time point and decreased faster than in the unblocked condition (30 min: Ø 26.1 %; 60 min: Ø 24.9 %). Taken together, FLT3 CAR-T cells form conjugates immediately after encountering target cells and keep the level of CAR-T cells involved in conjugates relatively stable over two hours of coculture. BiTE®-engaged T cells are not able to form as many conjugates with target cells as CAR-T cells in the beginning, but the level of BiTE®-engaged T cells in conjugates increases over time.

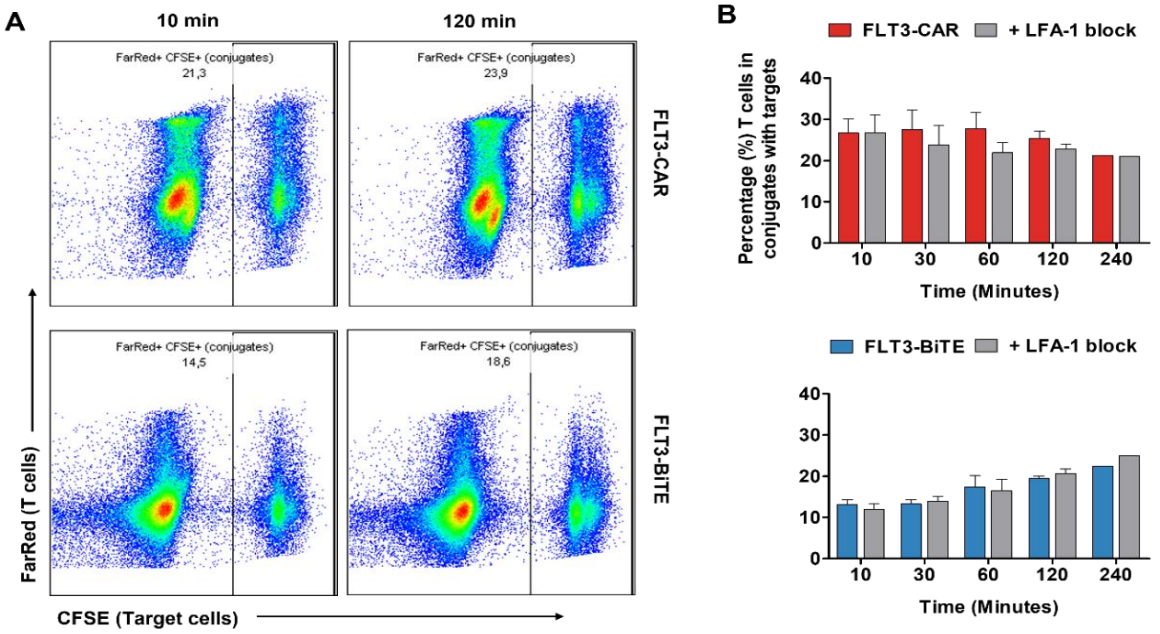

Figure 11: FLT3 CAR- and FLT3 BiTE®-mediated formation of conjugates with FLT3$^+$ target cells and the dependence on LFA-1 of stable immune synapses. A Percentage of CFSE$^+$FarRed$^+$ conjugates of total T cells after coculture with target cells for up to 2h with read out after 10, 30, 60, 120 and 240 min. FLT3 BiTE® concentration: 5 ng/ml. **B** LFA-1 was blocked on T cells (grey), unblocked T cells were used as control (colored). The cells were cultured as previously described (A). Percentage of CFSE$^+$FarRed$^+$ conjugates were determined by flow cytometry. Error bars represent mean +/- SEM. n=3.

3.4 CD107a T-cell degranulation as a rapid mechanism of FLT3 CAR-T and BiTE®-mediated antigen-specific cytotoxicity

FLT3 CAR-T cells showed noticeably higher CD107a fluorescence intensity already after 2h of stimulation with BA/F3-FLT3^{stong}CD86 cells compared to the isotype control, indicating degranulation (**Fig. 12A**). After 4 hours, there was no further increase. Also, FLT3 BiTE®-engaged T cells showed an increase of CD107a fluorescence intensity after 2h, but less pronounced than CAR-T cells. Again, there was no further increase after 4h. The MFI ratio of CD107a on CD3+ T cells was increasing until 4h and then decreased again on both CAR-T cells and BiTE®-engaged T cells, which indicates that CD107a degranulation happens rather at the beginning of coculture (**Fig. 12B**). The highest CD107a MFI ratios were observed for the CAR-T cells after 2h (Ø 6.20) and 4h (Ø 9.77), the MFI ratios for BiTE®-engaged T cells were initially a little lower (2h: Ø 3.42, 4h: Ø 6.36), but after 24h the values for CAR-T cells and BiTE-engaged T cells equalized (CAR: Ø 5.17, BiTE®: Ø 4.57) (**Fig. 12B**). These results suggest, that CD107a degranulation takes place rapidly after T cell-activation upon antigen-encounter, however, it does not remain at a consistently high level despite further stimulation by target cells and decreases again after 24h. Further, CAR-T cells mediate more rapid and more pronounced degranulation than BiTE®-engaged T cells.

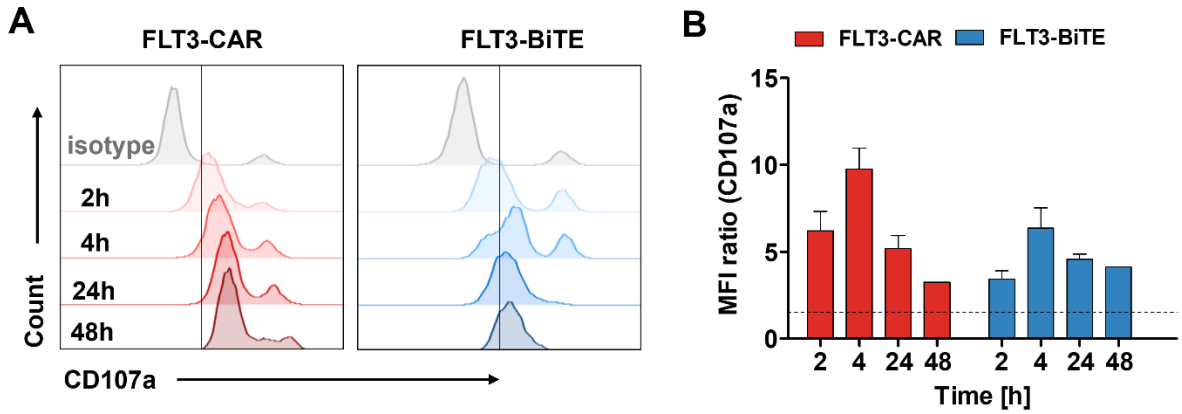

Figure 12: CD107a T-cell degranulation upon encounter of target-antigen by CAR-T or BiTE®-activated T cells. A Overlays of anti-CD107a and isotype signals of CD3$^+$ T cells determined by flow cytometry. FLT3 CAR-T cells (red) and FLT3 BiTE®-engaged HD T cells (blue) were cocultured with BA/F3-FLT3^{stong} cells for 24-48h and compared in their fluorescence intensity over time. BiTE® concentration 5 ng/ml. **B** MFI ratios of CD107a over time. The cells were cultured as previously described (A). Error bars represent mean +/- SEM. n=3.

3.5 CD86 costimulatory signal improves BiTE®-mediated TDCC

To evaluate, if the costimulatory signal of CD86 influences the CAR-T or BiTE®-mediated lysis of BA/F3-FLT3^{WT} or BA/F3-FLT3^{stong} cells, both cell lines were first transduced with CD86. To check the transduction efficiency, cells were stained for CD135, CD86 and viability and analyzed for CD135^{+}CD86^{+} double positive cells and sorted two times to get a higher purity. BA/F3-FLT3^{stong}CD86 and BA/F3-FLT3^{WT}CD86 were then used as target cells for a TDCC assay and BA/F3-FLT3^{stong} and BA/F3-FLT3^{WT} were used as control targets. At all E:T ratios, the presence of the CD86 costimulatory molecule led to an increase in the BiTE®-mediated lysis of both BA/F3-FLT3^{WT} and 'strong' cells (**Fig. 13**). At the E:T ratios 1:3 and 1:5, a significant increase was observed for the BiTE®-mediated lysis of BA/F3-FLT3^{WT}CD86 cells (~25 %) compared to BA/F3-FLT3^{WT} (~10 %) by a by two tailed Wilcoxon signed rank test (CI: 95 %). In comparison, CD86 costimulation had no impact on the CAR-mediated lysis, which was still overall higher (~30-60 %) than the BiTE®-mediated lysis (~10-40 %). With the FLT3 BiTE® construct, the BA/F3-FLT3^{stong} cells with a higher FLT3 expression were lysed better, no difference in the lysis between FLT3^{WT} and FLT3^{strong} cells was observed with CAR-T cells. These results suggest that the CAR-T-cell activity is hardly or not at all affected by the CD86 costimulation, while the activity of BiTE®-engaged T cells is more dependent on the CD86 costimulatory signal and can be increased by its presence.

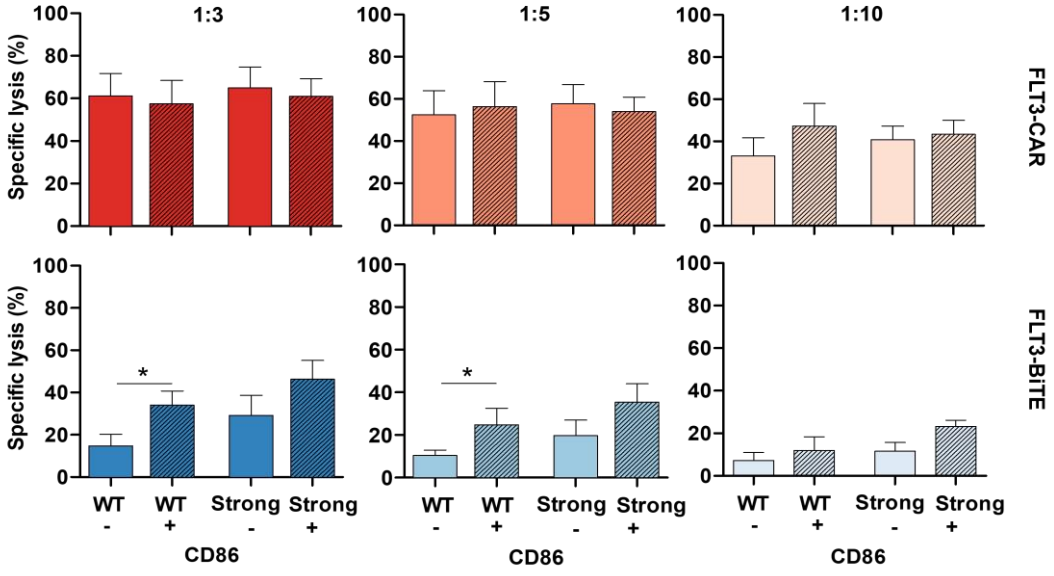

Figure 13: Influence of CD86 costimulation on the cytotoxic activity of FLT3 CAR-T and BiTE® construct. Specific lysis of FLT3 CAR-T and BiTE® construct against CD86^{+} or CD86^{-} Ba/F3-FLT3 cells. Target and effector cells were cocultured for 3 days at the indicated E:T ratio. BiTE® concentration: 5 ng/ml. Significance determined by two tailed Wilcoxon signed rank test, CI: 95 %. Error bars represent mean +/- SEM. n=6.

3.6 Combination with PD-1 blocking antibody Nivolumab enhances specific lysis of FLT3 CAR-T and BiTE® construct

MOLM13+PD-L1 were used for the PD-1 blocking experiment. The overall lysis on day 3 was higher with the FLT3 CAR-T construct (~40-60 %; BiTE®: ~25-55 %) (**Fig. 14A**). At an E:T ratio of 1:3, there was no difference in the lysis with or without the addition of Nivolumab in both CAR (Ø w: 62.9 %, w/o: 63.8 %) and BiTE® condition (Ø w: 53.5 %, w/o: 54.6 %).

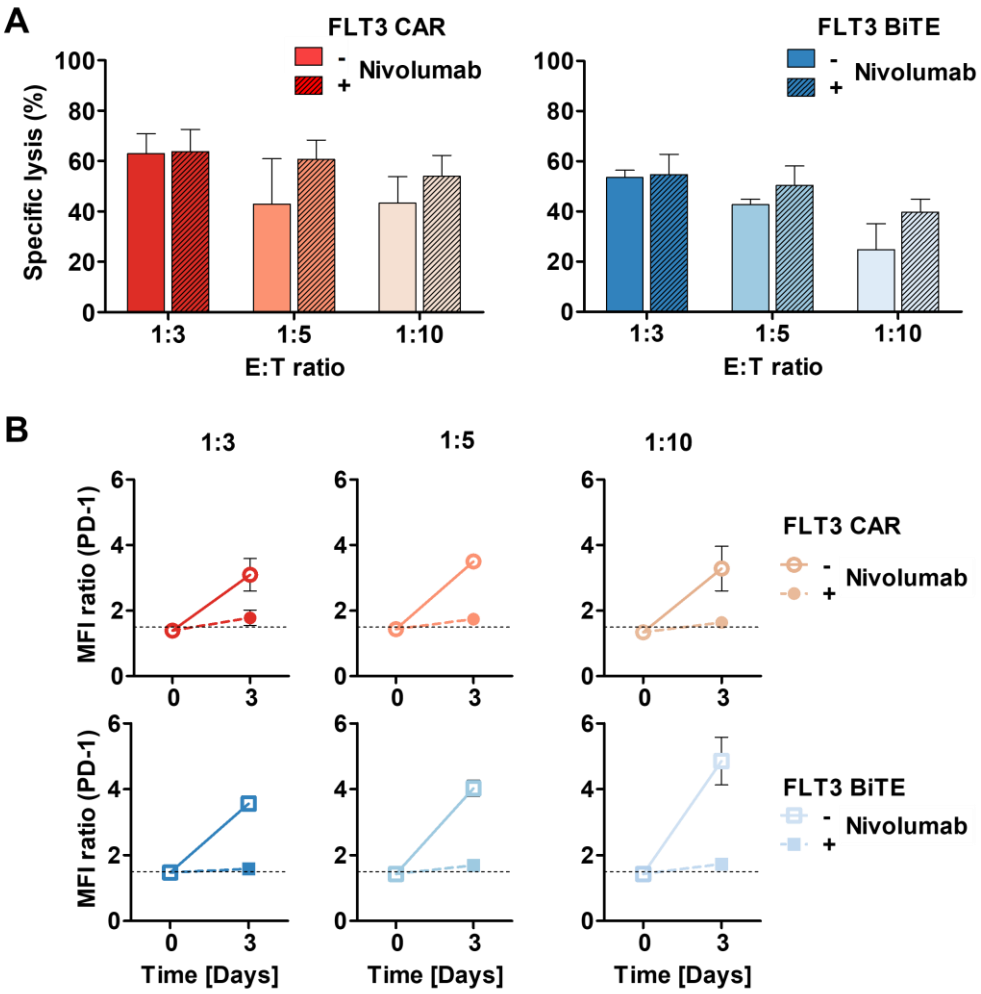

Figure 14: Influence of the PD-1 blocking antibody Nivolumab on the FLT3 CAR-T and BiTE®-mediated lysis. **A** Specific lysis mediated by FLT3 CAR-T (red) and BiTE® (blue) construct against MOLM13+PD-L1 cells with or without the addition of 10 µg/ml Nivolumab. Target and effector cells were co-cultured for 3 days at the indicated E:T ratio. A BiTE® concentration of 5 ng/ml was used. **B** MFI ratio of PD-1 was calculated based on PD-1 and isotype control MFI determined by flow cytometry. Expression on CAR-T (red) or BITE®-engaged T cells (blue) was compared between cultures with or without the addition of Nivolumab. Error bars represent mean +/- SEM. n=3.

In contrast, both CAR-T and BiTE®-mediated lysis was enhanced when Nivolumab was added to the cocultures with an E:T ratio of 1:5 (Ø CAR: +17.7 %, BiTE® +7.7 %) and 1:10 (Ø CAR: +10.6 %, BiTE® +14.9 %), but there was no significant enhancement. When Nivolumab was present, no upregulation of PD-1 on the surface of CAR-T cells and BiTE®-activated T cells was observed after 3 days of stimulation in coculture (MFI ratio CAR: ~1.7, BiTE®: ~1.6). Without the addition of Nivolumab, the PD-1 surface expression was upregulated on day 3 (MFI ratio CAR: ~3.2, BiTE®: ~4.1) (**Fig. 14B**). Expression of PD-1 on unblocked T cells increased in an E:T-dependent manner and was overall higher in the BiTE® setting. These results suggest that a combinational treatment of the FLT3 CAR-T or BiTE® therapy with PD-1 checkpoint inhibition could be beneficial for the patient.

3.7 Tyrosine kinase inhibitors modulate BiTE®-mediated lysis of MV4-11 cells

In previous experiments, the TKIs Quizartinib, Sorafenib and Gilteritinib were titrated on MOLM-13 (heterozygous FLT3 ITD/WT) and MV4-11 (homozygous FLT3 ITD/ITD) cells in context of a TDCC assay in combination with the FLT3 BiTE® construct (Brauchle et al. 2019). A high and a low concentration of the TKIs, that still affects the BiTE®-mediated lysis of the cell lines was determined. However, the results of an enhanced BiTE®- mediated lysis of MOLM-13 cells with additional TKI treatment could not be replicated by us. For the CAR-T setting, even a decrease in CAR-mediated lysis of MOLM-13 cells was found when the TKIs were added. Higher concentrations of the TKIs also lead to a more pronounced decrease of CAR-mediated lysis. A small increase in BiTE®-mediated lysis was observed for the low concentrations of Quizartinib and Sorafenib, while the higher concentrations also led to a decrease. Further, both concentrations of Gilteritinib lowered the BiTE®-mediated lysis (**Fig. 15A**). However, with the MV4-11 cells the previous results could be replicated and a dose-dependent increase in BiTE®-mediated lysis of MV4-11 cells has been observed with all three TKIs (**Fig. 15B**). The CAR-T mediated lysis of MV4-11 was again lowered when TKIs were added.

These results suggest that the combinational treatment of AML with the FLT3 BiTE® construct and both type I and II TKIs could enhance the killing of AML cells harboring a homozygous FLT3-ITD mutation. In contrast, the FLT3 CAR-T cell therapy does not seem to benefit from additional TKI treatment.

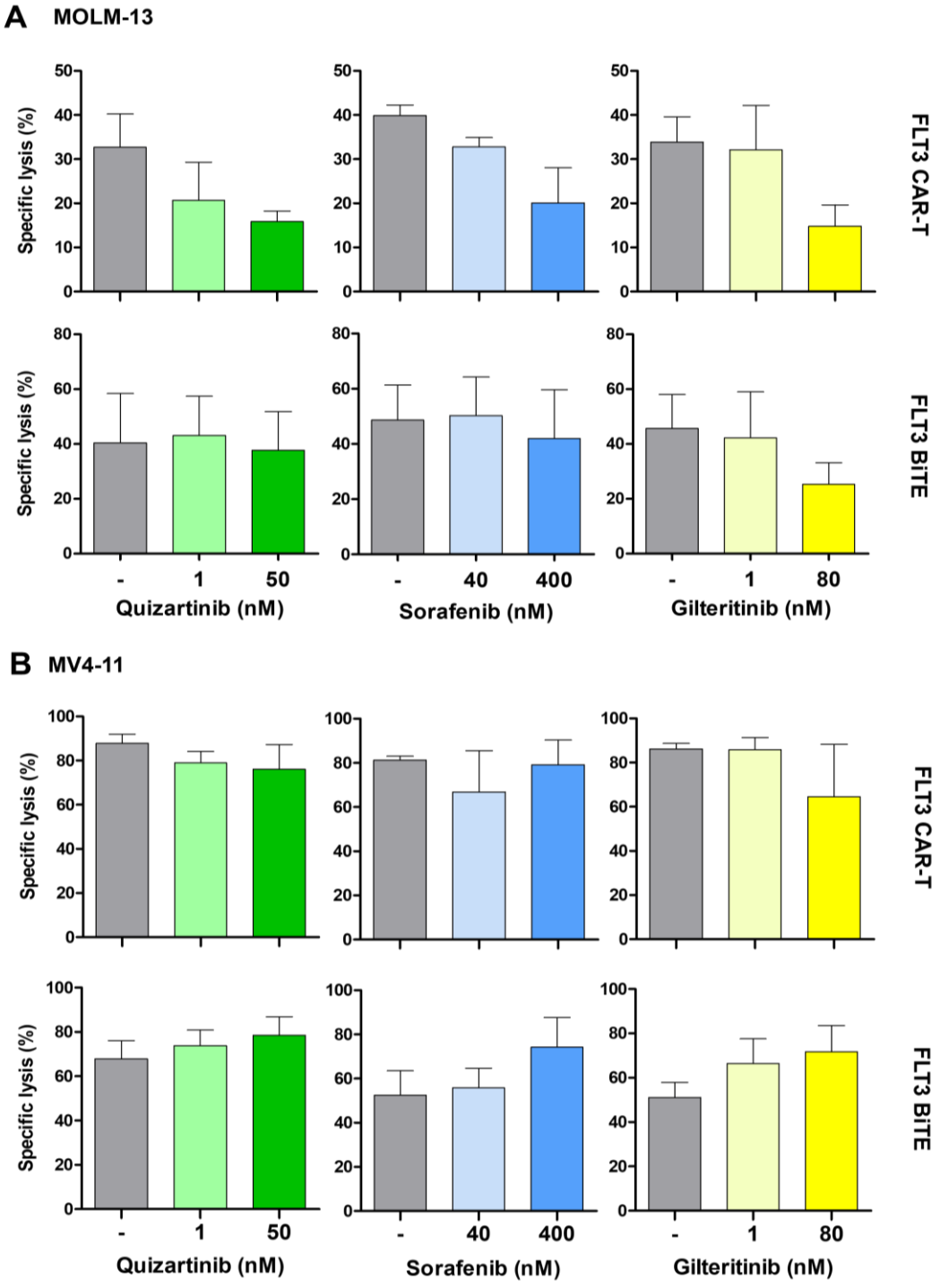

Figure 15: Modulating the activity of CAR-T/BiTE® through tyrosine kinase inhibitors (TKIs). A Specific lysis mediated by FLT3 CAR-T and BiTE® construct against MOLM-13 cells with (colored) and without (grey) the addition of TKIs. Green: Quizartinib, blue: Sorafenib, yellow: Gilteritinib. Target and effector cells were co-cultured for 3 days at an E:T ratio of 1:10, BiTE® concentration 5 ng/ml. Specific lysis was calculated based on $CD33^+$ cell. **B** Specific lysis mediated by FLT3 CAR-T and BiTE® construct against MV4-11 cells with (colored) and without (grey) the addition of TKIs. The cells were cultured as previously described (A). Error bars represent mean +/- SEM. n=3.

3.8 Bystander Killing mediated by FLT3 CAR-T cells and BiTE®

Target antigen-negative HEL 92.1.7 cells (bystander) cells were co-cultured with target antigen-positive MOLM-13 cells at different proportions, and CAR-T and BiTE®-mediated lysis of $FLT3^+$ or $FLT3^-$ cells was investigated. A high lysis of MOLM-13 cells was observed for both FLT3 CAR and BiTE®. Thereby, both CAR- (Ø 80 %) and BiTE®-mediated (Ø 83 %) lysis was the highest for the condition with only MOLM-13 cells without bystander cells, but no dose-dependent decrease of lysis was observed with decreasing proportions of MOLM-13 cells in the cocultures. The CAR-mediated lysis of HEL 92.1.7 bystander cells was overall low with about 4 % in the conditions with 25 % and 50 % HEL 92.1.7 and no lysis of bystander cells at all at higher proportions of HEL 92.1.7 cells in the coculture. In comparison to that, the BiTE®-mediated lysis of HEL 92.1.7 cells was higher. Thereby, the lowest lysis was observed in the condition with 25 % bystander cells (Ø 9 %) but increased noticeably in the conditions with 50 % and 75 % HEL 92.1.7 cells, with the highest lysis at 75 % bystander cells (Ø 38 %). The lysis of only HEL 92.1.7 without MOLM-13 was lower, with only Ø 13 % (**Fig. 16A**). These results demonstrate that BiTE®-engaged T cells are able to mediate a certain degree of bystander cell lysis while CAR-T cells are not. As the lysis of HEL 92.1.7 is lower in the condition with only HEL 92.1.7 cell but increases noticeably when they are cocultured with MOLM-13 cells, this clearly indicates a bystander effect. As this effect was suggested to rely on cytokine-mediated upregulation of ICAM-1 and FAS on target antigen-negative bystander cells (Ross et al. 2017), the expression of both antigens was measured on HEL 92.1.7 cells. Upon BiTE® treatment, there was only a moderate upregulation of FAS on HEL 92.1.7 in coculture with MOLM-13 cells (MFI ratios: Ø 4.7–6.7) compared to HEL 92.1.7 alone (MFI ratio: Ø 3.1). With only 25 % HEL 92.1.7 in coculture, the highest upregulation of FAS was observed (MFI ratio: Ø 6.7), for 50 % and 75 % it was lower. FAS expression on HEL 92.1.7 was also upregulated upon CAR-T cell treatment. MFI ratios were comparable with the BiTE® setting (**Fig. 16B**). ICAM-1 expression was strongly upregulated on HEL 92.1.7 in coculture with MOLM-13 upon BiTE® treatment. For HEL 92.1.7 alone, an MFI ratio of Ø 265 was calculated, while for the bystander setting the MFI ratios reached from Ø 1698-2983. The increase of ICAM-1 expression was highest in the condition with only 25 % HEL 92.1.7 (MFI ratio: Ø 2983) and decreased with higher proportions of HEL 92.1.7 cells in the cocultures. Again, also in the CAR setting a strong increase in ICAM-expression was observed, which was even higher than in the BiTE® setting (MFI ratios: Ø 2762-4590) (**Fig. 16C**).

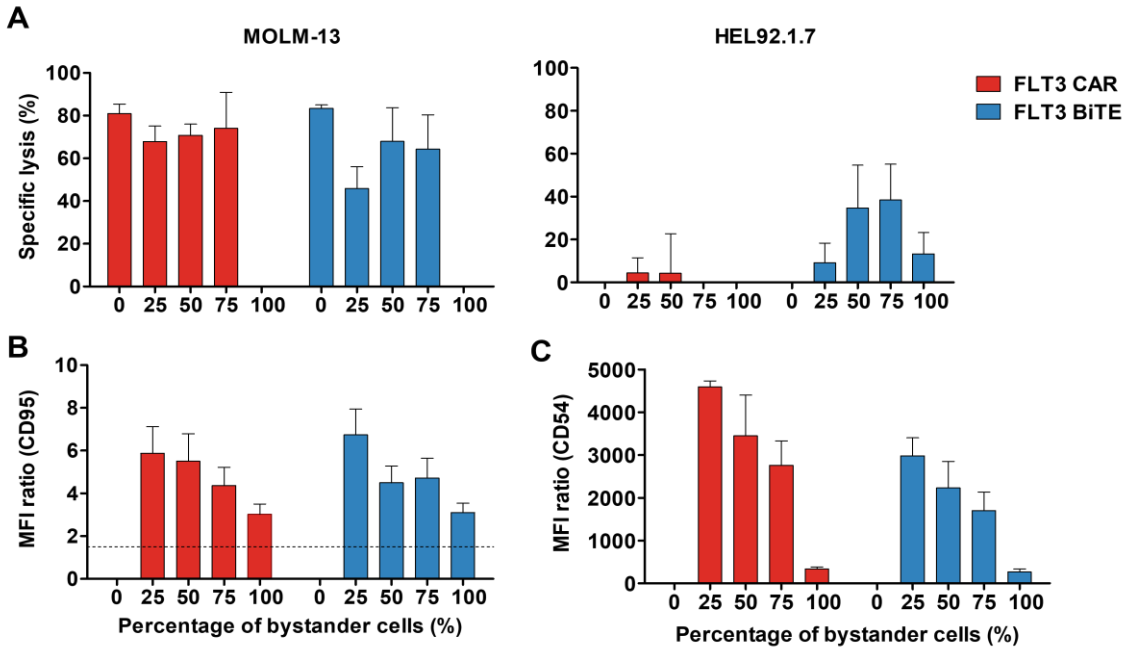

Figure 16: Bystander killing mediated by FLT3 CAR- or BiTE® construct and upregulation of FAS and ICAM-1 on bystander cells. A Specific lysis mediated by FLT3 CAR-T (red) and BiTE® (blue) against MOLM-13 cells and HEL 92.1.7 bystander cells. MOLM-13, HEL 92.1.7 and effector cells were co-cultured for 3 days at an E:T ratio of 1:3 with different proportion of bystander cells in the coculture, BiTE® concentration 5 ng/ml. Specific lysis was calculated based on CFSE+ or FarREd+ cell. **B** Surface expression of FAS displayed by MFI ratio. The cells were cultured as previously described (A). **C** Surface expression of ICAM-1 displayed by MFI ratio. The cells were cultured as previously described (A). Error bars represent mean +/- SEM. n=3.

3.9 Influence of Continuous Stimulation of CAR-T or BiTE®-activated T cells on their cytotoxic and proliferative potential

In a long-term coculture set up, proliferative and cytotoxic potential and T-cell exhaustion of both CAR-T cells and BiTE®-engaged T cell was investigated. Increased proliferation was observed in both cocultures until day 10 of continuous stimulation with Ba/F3-FLT3^{strong} cells, with a fold chance (FC) of Ø 1.57 for the CAR-T cells and Ø 2.54 for the BiTE®-activated T cells. In the following, T-cell proliferation decreased gradually until day 31 in both CAR (FC Ø 1) and BiTE® (FC Ø 0.7) setting (**Fig. 17A**). Cytotoxicity of both CAR-T cells and BiTE®-activated T cells also increased until day 10 of continuous stimulation (specific lysis CAR: Ø78 %; BiTE® 93 %) and stayed relatively stable at this level until day 24 in both settings. On day 31, target cell lysis decreased in both CAR (Ø 55 %) and BiTE® (Ø 82 %) treatment (**Fig. 17B**). PD-1 expression was upregulated upon every restimulation, but both interval of upregulation and basal PD-1 expression on CAR-T cells and BiTE®-engaged T cells becomes

lower over time (**Fig. 17C**). These results indicate that continuous stimulation with target-antigen expressing cells negatively impacts T-cell function in terms of their proliferative capacity and cytotoxicity because exhaustion of T cell takes place.

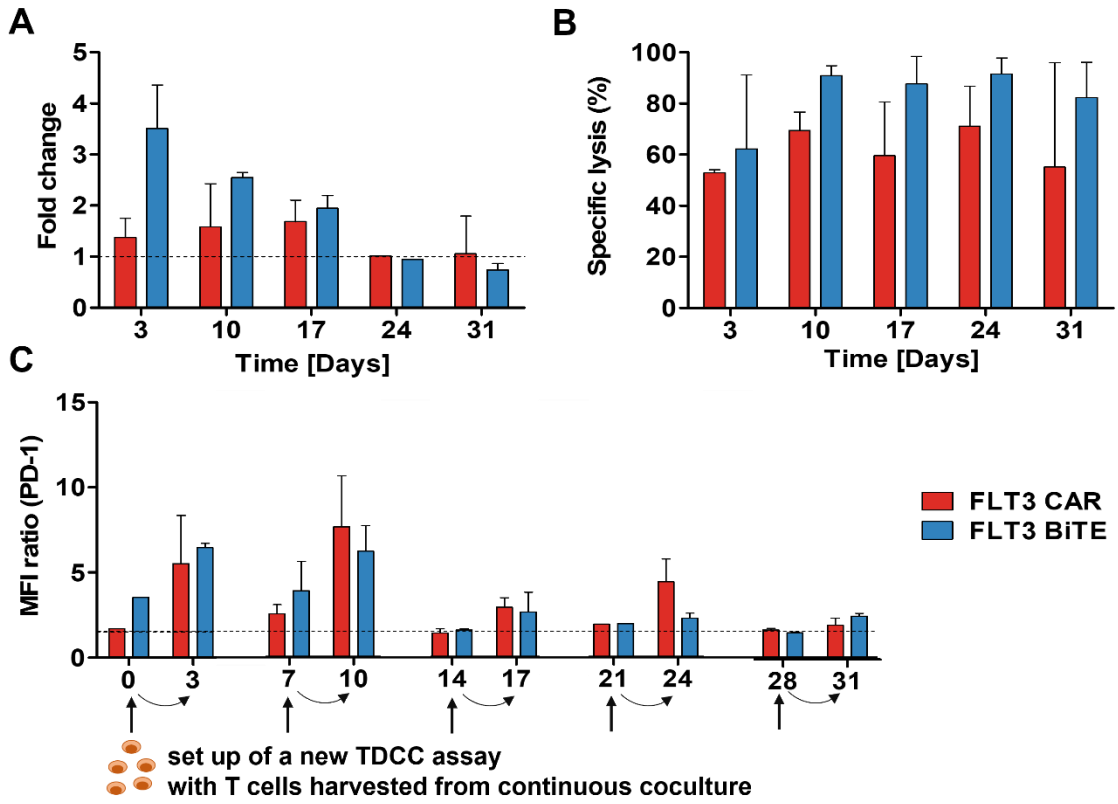

Figure 17: Influence continuous stimulation on FLT3 CAR-T cell and BiTE®-engaged T cell proliferation, cytotoxicity, and T cell-exhaustion. A Proliferation of FLT3 CAR-T (red) and BiTE®-engaged T cells (blue) over 31 days calculated by fold change of CD2 count every 7 days. **B** Specific lysis mediated by FLT3 CAR-T and BiTE® against Ba/F3 FLT3^{strong} cells. Target and effector cells were co-cultured for 3 days at an E:T ratio of 1:3, BiTE® concentration 5 ng/ml. **C** Surface expression of PD-1 on T cells displayed by MFI ratio over 31 days. The cells were cultured as previously described (B). Error bars represent mean +/- SEM. n=2.

3.10 FLT3 CAR-T cell and BiTE®-induced TDCC of healthy bone marrow *ex vivo*

Cytotoxicity of FLT3 CAR and BiTE® against healthy BMMCs was assessed. A higher lysis of healthy BMMCs at the E:T ratios 1:3 and 1:5 was observed for CAR-T cells (Ø 1:3 39.1 %; 1:5 24.9 %) compared to 5 ng/ml BiTE® (Ø 1:3 19.9 %; 1:5 10.0 %). At 1:10, a lysis of ~10 % BMMCs was observed with both FLT3 CAR-T cell and BiTE® treatment (**Fig. 18**). As FLT3 BiTE® shows a lower lysis of healthy bone marrow cells in this setting, treatment with the FLT3 BiTE® construct could be less harmful for healthy bone marrow cells.

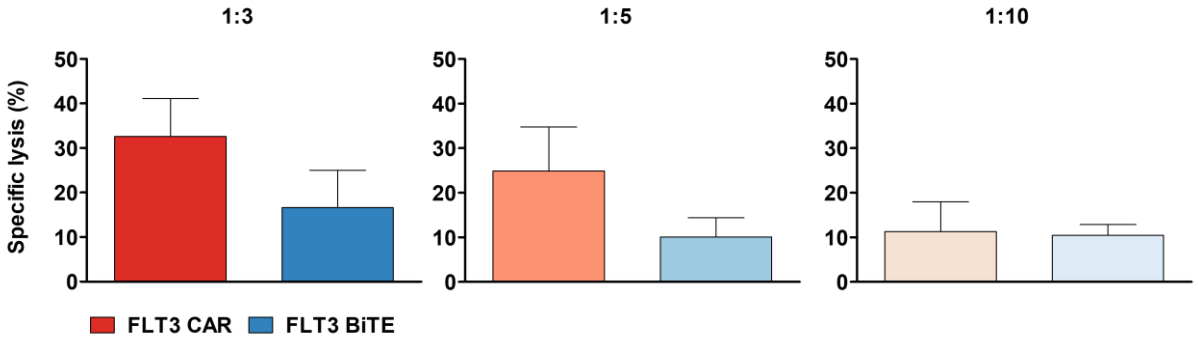

Figure 18: FLT3 CAR- and BiTE®-induced cytotoxicity against healthy bone marrow *ex vivo*. Specific lysis mediated by FLT3 CAR-T (red) and 5 ng/ml (blue) FLT3 BiTE® against healthy bone marrow monocytic cells. Cells were stained for CD2 and CD135 to distinguish cell populations. Error bars represent mean +/- SEM. n=6.

3.11 FLT3 CAR-T cell and BiTE®–induced TDCC of AML patient samples *ex vivo*

The efficacy of FLT3 CAR-T cells and BiTE® was assessed in the context of an *ex vivo* culture of pAML patient samples. After 3 days of coculture, CAR-T cell-mediated lysis was higher than BiTE®-mediated lysis at all E:T ratios. Highest lysis was observed at an E:T ratio of 1:3 for both CAR (Ø 65.6 %) and BiTE® (Ø 61.7 %) and lysis decreased in an E:T dependent manner to Ø 38.9 % CAR-mediated and Ø 34.9 % BiTE®-mediated lysis at an E:T ratio of 1:10. After 6 days, FLT3 BiTE®-mediated lysis (Ø 90 %) was higher than the lysis mediated by CAR-T cells (Ø 68.6 %) (**Fig. 19A**). Further, FLT3 surface expression on pAML blasts was investigated at the beginning and after 3 days of the coculture with T cells. An overall downregulation of FLT3 on the surface of pAML blasts was observed upon both CAR-T cell and BiTE® treatment in an E:T-independent manner. In the cocultures with CAR-T cells, downregulation of FLT3 was more pronounced than with BiTE® (**Fig. 19B**). The T-cell exhaustion marker PD-1 was upregulated on the surface of both CAR-T cells and BiTE®-engaged T cells after 3 days of coculture with pAML blasts. PD-1 surface expression increased E:T-dependent on both CAR-T cells and BiTE®-engaged T cells, but upregulation was more pronounced on BiTE®-engaged T cells (**Fig. 19C**). Taken together, both FLT3 CAR-T cells and BiTE® are able to mediate a potent killing of pAML blasts, indicating therapeutic benefits for AML patients. However, downregulation of FLT3 on the surface of pAML blasts and upregulation of PD-1 on T cells could reduce the therapeutic success, due to decreased T-cell function.

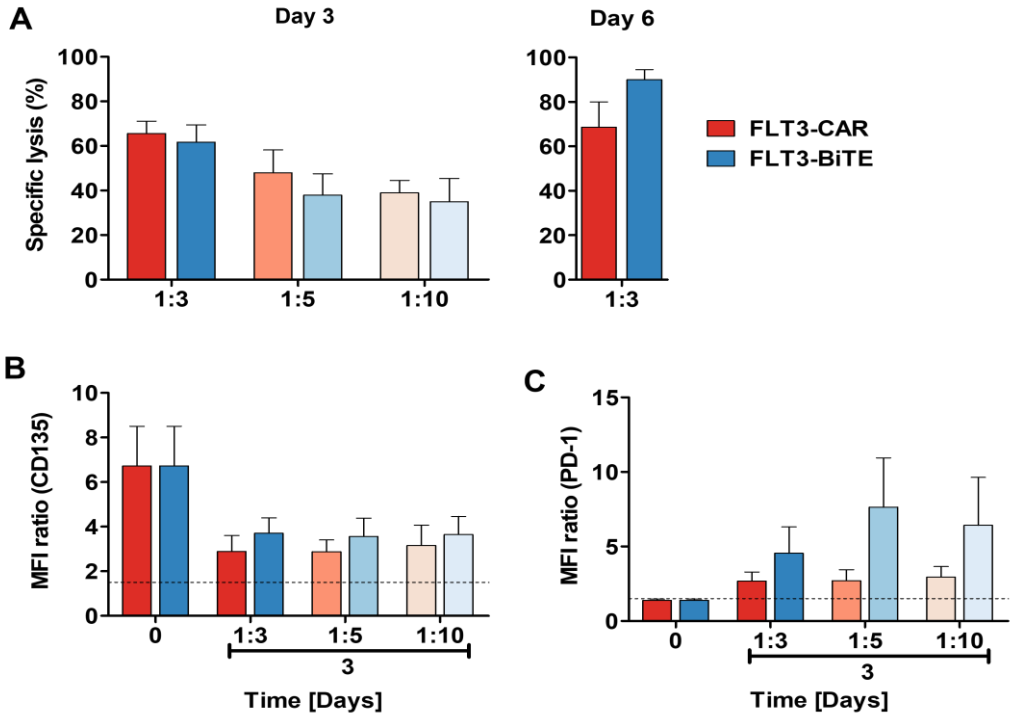

Figure 19: FLT3 CAR- and BiTE®-induced cytotoxicity against primary AML (pAML) patient samples *ex vivo*. **A** Specific lysis mediated by FLT3 CAR-T cells (red) and BiTE® (blue) against various pAML patient samples on day 3 and 5. **B** Surface expression of FLT3 on pAML blasts determined by MFI ratio on day 0 and 3 at different E:T ratios. The cells were cultured as previously described (B). **C** Surface expression of PD-1 on T cells determined by MFI ratio on day 0 and 3 at different E:T ratios. The cells were cultured as previously described (B). Error bars represent mean +/- SEM. Day 3 1:3 n=10, 1:5 n=6, 1:10 n=4. Day 6 n=5.

4 Discussion

For AML patients, intensive chemotherapy with or without allo-HSCT remains the mainstay of curative treatment, offering an extremely poor prognosis for intolerable, relapsed, or refractory patients (Sommer et al. 2020, Tabata et al. 2021). The FDA approved CD19-targeted blinatumomab (BiTE®) and tisagenlecleucel (tisa-cel, CAR) demonstrating that T-cell-based therapeutic strategies are capable of eliminating target antigen-expressing malignant cells with a high efficiency and thereby provide clinical benefits for patients suffering from hematologic malignancies (Brauchle et al. 2020, Tabata et al. 2021). Therefore, research aims to identify new leukemia-associated or specific antigens to develop further targeted therapeutic strategies. FLT3 was characterized as a suitable target for therapeutic applications, being expressed in leukemic cells with limited expression in healthy tissues (Daver et al. 2019, Ambinder and Levis 2021). In this project, an experimental FLT3 CAR- and FLT3 BiTE® construct were compared in terms of their efficacy and function.

FLT3 surface expression was assessed on mature hematopoietic cells isolated from healthy donors, and a low FLT3 surface expression was detected on all examined cell types (MFI ratios: 1.7-2.7). Further, a small portion of $FLT3^+$ cells was observed within each subpopulation (4.7-27 % $FLT3^+$ cells) and a shift of the whole population was observed for monocytes, dendritic cells and NK cells in our experiments, indicating that the whole population expresses FLT3 but only at a low level. This suggests that elimination of mature hematopoietic cells by the FLT3 CAR-T cell and BiTE® treatment is unlikely but cannot be completely ruled out. However, these results are contradictory to previous findings, where it was reported, that *FLT3* mRNA is not expressed in B and T lymphocytes and rarely expressed in monocytes and granulocytes (Rosnet et al. 1993). Only subsets of dendritic cells and natural killer cells were found to express FLT3 (Jetani et al. 2018). But overall, no FLT3 surface expression was reported in T or B lymphocytes, NK cells, dendritic cells or monocytes, indicating only a cytoplasmic FLT3 expression (Brauchle et al. 2020). Taken together it is further indicated in the literature, that FLT3-targeting CAR-T cell or BiTE® treatment is not anticipated to target mature hematopoietic cells, however our results indicate that on-target cytotoxicity of these cells cannot be completely ruled out.

First, FLT3 CAR-T cell and BiTE®-mediated lysis of $FLT3^+$ leukemic cell lines was evaluated *in vitro* for up to 6 days. Both constructs demonstrated potent TDCC against human $FLT3^+$ leukemic cell lines. Overall, BiTE® treatment mediated a higher killing than CAR-T cells. To

prove, that the lysis of the FLT3^{+} cell lines was indeed FLT3-specific, TDCC against a FLT3^{-} cell line was assessed. FLT3 unspecific BiTE®-mediated lysis was overall low with a maximum of 10 % lysed cells, while CAR-T cell did not mediate unspecific lysis of FLT3^{-} cells at all.

Further, the ability of FLT3 CAR-T cells and BiTE®-engaged T cells to form conjugates with target cells and to mediate degranulation upon engagement of FLT3^{+} cells were assessed. Again, both FLT3 CAR- and BiTE®-construct formed conjugates with target cells, indicating stable immune synapse formation. Also, both constructs mediated degranulation, assessed by CD107a MFI ratios. However, conjugates formation and degranulation were observed to happen more rapidly in cocultures with FLT3 CAR-T cells than with BiTE®-engaged T cells. This observation agrees with literature, where it was reported, that CAR-T cells form nonclassical immune synapses. This is related to a more rapid synapse-initiated signaling in CAR-T cells, leading to faster degranulation and to a shorter duration of conjugate formation enabling a fast serial killing (Davenport et al. 2018). In contrast, BiTE®-engaged T cells must first be activated upon encountering target cells and form an immune synapse that is more similar to the classical TCR synapses. Therefore, they need more time to form stable conjugates und mediate target cell killing (Offner et al. 2006). Further our results suggest, that FLT3 CAR-T cells were negatively affected by LFA-1 blocking in their ability to form conjugates, while BiTE®-engaged T cells were not affected at all. These results need to be further elucidated as they are contradictory to pervious findings, where evidence was gained that the differences in the synapse formation make BiTE®-engaged T cells more dependent on LFA-1, as they form an organized pSMAC and require LFA-1 for the stabilization of the synapse. On the other hand, CAR-T cells form a disorganized synapse lacking a defined structure and do not need LFA-1 for stabilization (Strohl and Naso 2019).
It cannot be ruled out, that the decreasing MFI ratios of CD107a in cocultures with both FLT3 CAR-T cells and BiTE® after 24-48 h do not result from reduced degranulation, but from continuous intracellular trafficking of CD107a, as intracellular protein transport was not blocked in this assay. It was recently reported that with the addition of an intracellular protein transport inhibitor, a peak response of CD107a was detected at 48 h in BiTE®-engaged T cells (Frank et al. 2018). In order to detect the full extent of degranulation it could be therefore beneficial to also include an intracellular protein transport inhibitor in our assay set up in the future.

CAR-constructs are designed to be able to function independently of a costimulatory “signal 2” as they already contain intracellular costimulatory signaling domains and therefore provide the costimulatory signals by themselves. However, effector function and targeted killing of BiTE®-

engaged T cells can be enhanced by costimulatory molecules (Strohl and Naso 2019). In line with this, an enhanced killing of $FLT3^{+}$ target cells mediated by FLT3 BiTE® engaged T cells was observed when the costimulatory molecule CD86 was present on the surface of target cells. In contrast, the killing capacity of FLT3 CAR-T cells was not influence by CD86 target cell expression.

Further, CAR-mediated lysis seems to be less dependent on the FLT3 expression level, while the BiTE®-mediated lysis increases with higher FLT3 expression on BA/F3-FLT3 cells. These findings are contrary to the observed lysis of MV4-11, MOLM-13 and OCI-AML3 cells where also the BiTE®-mediated lysis not clearly correlated with the FLT3 expression. However, the difference between the FLT3 surface expression levels on the BA/F3-$FLT3^{stong}$CD86 (MFI ratio: Ø 170) compared to BA/F3-$FLT3^{WT}$CD86 (MFI ratio: Ø ~60) is much higher than the differences between MV4-11, MOLM-13 and OCI-AML3 cells (MFI ratios: Ø 1.67-6.38).

An increased frequency of PD-1 positive T cells was observed in patients with AML compared with healthy individuals and showed to increase upon relapse, suggesting an exhausted T cells status (Williams et al. 2019). In 25 % of AML CD34+ and 32 % of AML PBMC samples, PD-L1 mRNA expression was upregulated compared to healthy donors (Yang et al. 2014). To counteract the upregulation of these inhibitory immune checkpoint molecule, various publications have substantiated that combination therapy with checkpoint inhibitors can enhance both CAR- and BiTE®-mediated T-cell killing and retard T-cell exhaustion (Krupka et al. 2016, Chang et al. 2017, Song and Zhang 2020). Indeed, combinatorial treatment with the PD-1 blocking antibody nivolumab also enhances the therapeutic efficacy of both FLT3 CAR and BiTE® construct against PD-L1 expressing MOLM-13 cell. Further, no upregulation of the T-cell exhaustion marker PD-1 was observed on the T cell surface upon treatment with nivolumab, however we suppose that binding of nivolumab to PD-1 blocks the binding of the staining antibody and therefore no increased PD-1 surface expression was detectable.

FLT3 TKIs have already shown efficiency in clinical trials but are prone to resistance, wherefore combination therapy is recommended. For the FLT3 BiTE® construct, an increase in homozygous FLT3-ITD/ITD target cell killing was observed, when the TKIs Quizartinib, Sorafenib and Gilteritinib were added to the coculture. However, this effect could not be shown for heterozygous FLT3-ITD/WT target cells, where lysis overall decreased upon addition of TKIs. It was ruled out that the TKIs had a negative effect on the T cells, wherefore the beneficial effect of TKI addition might be dependent on the mutational status of the target cells. FLT3

CAR-mediated killing of both homozygous and heterozygous target cells did not benefit from additional TKI treatment in our experiments.

A potential challenge for targeted therapy strategies is the heterogeneity of TAA expression, that serves as a potential source of resistance, especially in solid tumors. Therefore, a desirable treatment modality is the killing of both TAA-positive malignant cells, as well as proximal TAA-negative cells (bystanders) in order to prevent escape and outgrowth of TAA-negative clones during treatment. This effect can be mediated by the upregulation of the adhesion molecule ICAM-1 and the death receptor FAS on bystander cells upon IFNγ and TNF secretion of T cells, leading to a more stabilized cytolytic synapse formation and enhanced death receptor signaling (Ross et al. 2017). Recently, evidence for bystander killing was provided for both BiTE®- and CAR-constructs (Ross et al. 2017, Lanitis et al. 2012). In our experiments, only the FLT3 BiTE®-engaged T cells were able to kill both $FLT3^+$ target and $FLT3^-$ bystander cells, while the FLT3 CAR-T cells could not mediate killing of bystander cells at all. Despite these differences, both FLT3 CAR and BiTE® treatment led to the upregulation of ICAM-1 and FAS on bystander cells, when they are in coculture with $FLT3^+$ target cells. The fact that the CAR-T cells do not lyse the HEL 92.1.7 as efficiently as the BiTE® in the bystander setting, although FAS and ICAM-1 are upregulated to a similar extend could be explained by the nonclassical immune synapses formed by CAR-T cells that are largely independent of LFA-1/ICAM-1 interactions. This means that a higher ICAM-1 expression on bystander cells does not directly contribute to more stable synapse formation between CAR-T cells and HEL 92.1.7 cells, as it is the case for BiTE®-mediated synapses and could thus explain the difference in bystander lysis between FLT3 CAR and BiTE®.

When mimicking continuous stimulation of FLT3 CAR-T cells and BiTE®-engaged T cells by a long-term coculture *in vitro*, it was shown, that cytotoxic and proliferative potential first increases, but over long-term stimulation, both proliferative capacity and cytotoxicity decrease over time. This indicates that continuous stimulation with $FLT3^+$ target cells negatively impacts both CAR- and BiTE-engaged T-cell function over time. It was recently shown for BiTE therapy, that treatment-free interval can mitigate T-cell exhaustion and restore T-cell function (Zieger et al. 2020). This is another advantage of BiTE® constructs because their short half-life enables treatment interruptions or discontinuation if necessary. In contrast, it is difficult to “stop” CAR-T cell treatments because of their expansion and persistence *in vivo*. This is also important in management of adverse events, where pharmacological immunosuppression is needed for CAR-T cell therapy, while BiTE® treatment can be adjusted or interrupted anytime during

treatment (Subklewe 2021). However, various approaches to enable a better regulation of CAR-T cells have been established in the recent years, for example by introducing a pharmacologic on/off switch (Sommer et al. 2020, Mestermann et al. 2019).

It is a common issue of targeted therapy approaches, that they not only lead to the elimination of malignant cells, but also to a collateral loss of healthy cells regrown from unaffected healthy hematopoietic stem and progenitor cells (Myburgh et al. 2020). As FLT3 is expressed on hematopoietic cells at different stages of differentiation, it is likely that also healthy hematopoietic stem and progenitor cells are getting killed by FLT3 CAR and BiTE® constructs. Indeed, both FLT3 CAR and BiTE® mediated a low killing of healthy bone marrow cells. However, alloreactivity of T cells against the healthy bone marrow may have also played a role in this set up, as the T cells were derived from different donors than the bone marrow samples. An advantage of BiTE® constructs in this context is that the administered concentration can be adjusted to mitigate unwanted effects. Therefore, FLT3 BiTE® treatment could be the better choice to achieve recovery of healthy bone marrow cells during the therapy.

By assessing TDCC against *ex vivo* cultured pAML patient samples, both FLT3 CAR- and BiTE® construct could induce potent lysis of AML blasts after 3 and 6 days of coculture, indicating therapeutic efficacy in patients. However, what could be an issue for FLT3-targeted therapies, is the observation that surface FLT3 was downregulated on all pAML blasts already after 3 days of treatment with FLT3 CAR- or BiTE®. This could lead to treatment escape of $FLT3^{low}$ clones and lead to resistance against FLT3-targeted therapies. Further, PD-1 was upregulated on both CAR-T cells and BiTE®-engaged T cells upon coculture with pAML blasts, indicating T-cell exhaustion already after 3 days of treatment.

Apart from these results, it is stated in literature that BiTE® treatment also benefits from the simple recombinant production and purification, whereby an off-the-shelf availability is possible. Further, the low molecular weight of BiTE® molecules enables tissue penetration (Slaney et al. 2018). CAR-T cells are engineered for each patient individually and require several steps of production, making it expensive and time consuming. Even though the production process is well established, each step carries the possibility of error, leading to ≤10 % of patients not receiving the CAR-treatment due to manufacturing failure (Subklewe 2021).

Taken together, both our own results and recent findings by others indicate, that the FLT3 BiTE® construct might be the better choice for the treatment of AML. It is easier to use, can be

adapted to the therapy progress and induces a potent target specific lysis of $FLT3^+$ cells. Further, it is less cytotoxic against healthy bone marrow cells, enabling a better bone marrow recovery. In contrast to FLT3 CAR-T cells, FLT3 BiTE® therapy can benefit of combinational treatments with both PD-1 blocking antibodies and FLT3 TKIs and can mediate bystander killing.

5 Zusammenfassung

Patienten, die an akuter myeloischer Leukämie (AML) leiden, erhalten immer noch eine schlechte klinische Prognose, was den Bedarf an neuen oder verbesserten Therapien untermauert (Wang et al. 2018, Brauchle et al. 2020). Gentechnisch hergestellte chimäre Antigenrezeptor (CAR) T-Zellen, die die Antigenerkennung eines Antikörpers und die langfristigen Effektorfunktionen von T-Zellen kombinieren, konnten bereits klinische Erfolge bei der Behandlung der akuten lymphatischen Leukämie (ALL) erzielen (Wang et al. 2018, Hofmann et al. 2019). Bispezifische T-Zell-Engager-Konstrukte (BiTE®) leiten T-Zellen um, sodass sie gezielt Tumorzellen abtöten, und ihr Erfolg wurde ebenfalls schon bei hämatologischen Malignomen klinisch validiert (Huehls et al. 2015). Aufgrund der hohen Expressionsraten auf AML-Blasten und der begrenzten Expression in normalem Gewebe gilt die FMS-ähnliche Tyrosinkinase 3 (FLT3) als geeignetes tumorassoziiertes Antigen und wurde in letzter Zeit sowohl als Ziel für CAR- als auch für BiTE®-Konstrukte verwendet (Gilliland and Griffin 2002, Brauchle et al. 2020). Um die Wirksamkeit und Funktion eines FLT3 CAR- und eines FLT3 BiTE®-Konstrukts zu bewerten und zu vergleichen, wurde die T-Zell abhängige zelluläre Zytotoxizität (TDCC) gegen FLT3-positive Zelllinien *in vitro* oder primäre AML (pAML)-Blasten *ex vivo*, sowie die unspezifische Lyse und die Erschöpfung der T-Zellen bewertet. Während die FLT3 BiTE® Behandlung im Vergleich zur CAR-T Zell Behandlung eine höhere spezifische Lyse von FLT3-positiven Zelllinien zeigte, konnten CAR-T Zellen nach 3 Tagen eine höhere Lyse von pAML Spenderproben erzielen. CAR-T-Zellen zeigten in gesundem Knochenmark eine höhere unspezifische Lyse, während bei der Behandlung mit dem FLT3 BiTE® eine höhere Lyse von FLT3-negativen Zelllinien beobachtet wurde. Durch die Ko-Kultur mit Tumorzellen wurde PD-1 auf BiTE® gebundenen T-Zellen stärker hochreguliert, während sowohl die CAR- als auch die BiTE®-Behandlung zu einer Herunterregulierung von FLT3 auf Zelllinien und pAML-Blasten führten. Die Kombination mit dem PD-1-blockierenden Antikörper Nivolumab erhöhte sowohl die CAR- als auch die BiTE®-vermittelte Lyse, während die Zugabe von Tyrosinkinase-Inhibitoren nur einen positiven Effekt auf die BiTE®-Aktivität hatte. Zusammenfassend lassen diese *in vitro*-Ergebnisse für keine der beiden Therapieformen eindeutige Vorteile erkennen. Generell wird jedoch ein Vorteil für BiTE®-Konstrukte gesehen, da die Herstellung von CAR-T-Zellen mehrere Wochen dauert und oft scheitert, während BiTE®-Antikörper „von der Stange“ erhältlich sind. Darüber hinaus ist die Gabe von BiTE®-Antikörpern in wiederholter Dosierung möglich und die Behandlung kann unterbrochen werden, was für CAR-T-Zellen komplizierter ist.

6 Abstract

Patients suffering from acute myeloid leukemia (AML) still face a poor clinical prognosis, underpinning the need for novel or improved therapies (Brauchle et al. 2020, Wang et al. 2018). Genetically engineered chimeric antigen receptor (CAR) T cells, which combine the target recognition of an antibody and the long-term effector function of T cells, have already achieved clinical success in the treatment of acute lymphoblastic leukemia (ALL) (Hofmann et al. 2019, Wang et al. 2018). Bispecific T cell engager (BiTE®) constructs redirect T cells to promote targeted killing of tumor cells and their success have been clinically validated in hematologic malignancies (Huehls et al. 2015). Due to its high expression levels on AML blasts and the limited expression on normal tissue, the FMS-like tyrosine kinase 3 (FLT3) is considered a suitable tumor associated antigen and was lately used as a target for both CAR- and BiTE®-constructs (Gilliland and Griffin 2002, Brauchle et al. 2020). To evaluate and compare the efficacy and function of a FLT3 CAR and a FLT3 BiTE® construct, T-cell–dependent cellular cytotoxicity against FLT3-positive cell lines *in vitro* or primary AML (pAML) blasts *ex vivo*, off-target lysis and T-cell exhaustion was assessed. While treatment with FLT3 BiTE® molecule showed a higher specific lysis of FLT3-positive cell lines compared to CAR-T cell treatment, a higher lysis of pAML samples was observed with CAR-T cells after 3 days of coculture. CAR-T cell treatment showed a higher off target lysis on healthy bone marrow, while treatment with the BiTE® reached a higher lysis of FLT3-negative cell lines, also in a bystander setting. Upon treatment, PD-1 on T cells was upregulated to a higher extend in the BiTE® condition, while both FLT3 CAR-T cell and BiTE® treatment led to a downregulation of FLT3 on cell lines and pAML blasts. Combination with the PD-1 blocking antibody Nivolumab increased both CAR- and BiTE®- mediated lysis, while the addition of tyrosine kinase inhibitors only had a positive effect on the BiTE® activity. In summary, these *in vitro* results do not reveal any clear advantages for either of the two therapy forms. However, in general an advantage is seen for BiTE® constructs, since the manufacturing of CAR-T cells takes several weeks and often fails, while BiTE® antibodies are available “off-the-shelf”. Further, BiTE® administration is possible in repetitive dosing and the treatment can be interrupted, which is more complicated for CAR-T cells.

7 Table of abbreviations

ALL ..... *Acute lymphoblastic leukemia*
allo-HSCT ..... *Allogenic hematopoietic stem cell transplantation*
AML ..... *Acute myeloid leukemia*
APC ..... *Antigen presenting cell*
BiTE ..... *Bispecific T-cell engager*
BM ..... *Bone marrow*
BMMC ..... *Bone marrow mononuclear cells*
$CaCl_2$ ..... *Calciumchlorid*
CAR ..... *Chimeric antigen receptor*
cBiTE ..... *Control BiTE*
CLL ..... *Chronic lymphoblastic leukemia*
CML ..... *Chronic myelogenous leukemia*
CR ..... *Complete remission*
CRES ..... *CAR T cell-related encephalopathy syndrome*
CRS ..... *Cytokine release syndrome*
cSMAC ..... *Central supramolecular activation cluster*
CTLA-4 ..... *Cytotoxic T lymphocyte-associated antigen-4*
DMEM 1x ..... *Dulbecco's modified eagle medium*
DPBS ..... *Dulbecco's phosphate-buffer saline*
dSMAC ..... *Distal supramolecular activation cluster*
E:T ..... *Effector to target cell ratio*
FBS ..... *Fetal bovine serum*
FLT3 ..... *FMS-like tyrosine kinase 3*
HD ..... *Healthy donor, Healthy donor*
HSC ..... *Hematopoietic stem cell*
IS. ..... *Immune synapse*
ITD ..... *Internal tandem duplication*
LAA ..... *Leukemia associated antigen*
LAG-3 ..... *Lymphocyte-activated gene 3*
LSA ..... *Leukemia-specific antigen*
mAb ..... *Monoclonal antibody*
MFI ..... *Mean fluorescence intensity*

MHC ..... Major histocompatibility complex
MRD ..... Measurable residual disease
NPM1 ..... Nucleophosmin 1
P.Eco ..... Phoenic-ECO
pAML ..... primary AML
PBMC ..... Pheripheral blood mononuclear cells
PD-1 ..... Programmed cell death protein 1
PD-L1 ..... Programmed death ligand 1
PSG ..... Penicillin-Streptomycin-Glutamine
pSMAC ..... Peripheral supramolecular activation cluster
scFv ..... single chain fragment variable
SMAC ..... Supramolecular activation cluster
ßME ..... ß-Mercaptoethanol
TAA ..... Tumor-associated antigen
T_{CM} ..... Central memory T cell
TCR ..... T-cell receptor
TDCC ..... T-cell dependent cellular cytotoxicity
T_{EFF} ..... Effector T cell
T_{EM} ..... Effector memory T cell
TIM3 ..... T cell immunoglobulin and mucin domain-containing protein 3
TKD ..... Tyrosine kinase domain
TKI ..... Tyrosine kinase inhibitor
T_N ..... Naive T cell
TRUCK ..... T-cells redirected for universal cytokine-mediated killing
T_{SCM} ..... Stem cell memory T cell
UT ..... Untransduced T cell

8 References

Aldoss I, Bargou RC, Nagorsen D, Friberg GR, Baeuerle PA, Forman SJ. 2017. Redirecting T cells to eradicate B-cell acute lymphoblastic leukemia: bispecific T-cell engagers and chimeric antigen receptors. Leukemia, 31 (4):777-787.

Ambinder AJ, Levis M. 2021. Potential targeting of FLT3 acute myeloid leukemia. Haematologica, 106 (3):671-681.

Anguille S, Van Tendeloo VF, Berneman ZN. 2012. Leukemia-associated antigens and their relevance to the immunotherapy of acute myeloid leukemia. Leukemia, 26 (10):2186-2196.

Brauchle B, Goldstein RL, Chi-Ming L, Buecklein V, Krupka C, Koppikar P, Haubner S, Thomas O, Rock DA, Sastri C, Cooke K, von Bergwelt-Baildon M, Metzeler KH, Spiekermann K, Arvedson TA, Subklewe M. 2019. Targeting FLT3 In AML: Modulation of FLT3-BITE® Activity through Combination with various TKI. EHA Library.

Brauchle B, Goldstein RL, Karbowski CM, Henn A, Li CM, Bucklein VL, Krupka C, Boyle MC, Koppikar P, Haubner S, Wahl J, Dahlhoff C, Raum T, Rardin MJ, Sastri C, Rock DA, von Bergwelt-Baildon M, Frank B, Metzeler KH, Case R, Friedrich M, Balazs M, Spiekermann K, Coxon A, Subklewe M, Arvedson T. 2020. Characterization of a Novel FLT3 BiTE Molecule for the Treatment of Acute Myeloid Leukemia. Mol Cancer Ther, 19 (9):1875-1888.

Chang CH, Wang Y, Li R, Rossi DL, Liu D, Rossi EA, Cardillo TM, Goldenberg DM. 2017. Combination Therapy with Bispecific Antibodies and PD-1 Blockade Enhances the Antitumor Potency of T Cells. Cancer Res, 77 (19):5384-5394.

Chao MP, Seita J, Weissman IL. 2008. Establishment of a normal hematopoietic and leukemia stem cell hierarchy. Cold Spring Harb Symp Quant Biol, 73:439-449.

Cheever MA, Allison JP, Ferris AS, Finn OJ, Hastings BM, Hecht TT, Mellman I, Prindiville SA, Viner JL, Weiner LM, Matrisian LM. 2009. The prioritization of cancer antigens: a national cancer institute pilot project for the acceleration of translational research. Clin Cancer Res, 15 (17):5323-5337.

Davenport AJ, Cross RS, Watson KA, Liao Y, Shi W, Prince HM, Beavis PA, Trapani JA, Kershaw MH, Ritchie DS, Darcy PK, Neeson PJ, Jenkins MR. 2018. Chimeric antigen receptor T cells form nonclassical and potent immune synapses driving rapid cytotoxicity. Proc Natl Acad Sci U S A, 115 (9):E2068-E2076.

Daver N, Schlenk RF, Russell NH, Levis MJ. 2019. Targeting FLT3 mutations in AML: review of current knowledge and evidence. Leukemia, 33 (2):299-312.

De Kouchkovsky I, Abdul-Hay M. 2016. 'Acute myeloid leukemia: a comprehensive review and 2016 update'. Blood Cancer J, 6 (7):e441.

Esfahani K, Roudaia L, Buhlaiga N, Del Rincon SV, Papneja N, Miller WH, Jr. 2020. A review of cancer immunotherapy: from the past, to the present, to the future. Curr Oncol, 27 (Suppl 2):S87-S

Frank B, Wei Y, Kim K, Guerrero A, Lebrec H, Balazs M, Wang X. 2018. Development of a BiTE®-mediated CD8+ cytotoxic T-lymphocyte activity assay to assess immunomodulatory potential of drug candidates in Cynomolgus macaque. Journal of Immunotoxicology 15 (1):119-125.

Gilliland DG, Griffin JD. 2002. The roles of FLT3 in hematopoiesis and leukemia. Blood, 100 (5):1532-1542.

Grupp SA, Kalos M, Barrett D, Aplenc R, Porter DL, Rheingold SR, Teachey DT, Chew A, Hauck B, Wright JF, Milone MC, Levine BL, June CH. 2013. Chimeric antigen receptor-modified T cells for acute lymphoid leukemia. N Engl J Med, 368 (16):1509-1518.

Hofmann S, Schubert ML, Wang L, He B, Neuber B, Dreger P, Muller-Tidow C, Schmitt M. 2019. Chimeric Antigen Receptor (CAR) T Cell Therapy in Acute Myeloid Leukemia (AML). J Clin Med, 8 (2).

Huehls AM, Coupet TA, Sentman CL. 2015. Bispecific T-cell engagers for cancer immunotherapy. Immunol Cell Biol, 93 (3):290-296.

Hurton LV, Singh H, Najjar AM, Switzer KC, Mi T, Maiti S, Olivares S, Rabinovich B, Huls H, Forget MA, Datar V, Kebriaei P, Lee DA, Champlin RE, Cooper LJ. 2016. Tethered IL-15 augments antitumor activity and promotes a stem-cell memory subset in tumor-specific T cells. Proc Natl Acad Sci U S A, 113 (48):E7788-E7797.

Itoh K, Tezuka H, Sakoda H, Konno M, Nagata K, Uchiyama T, Uchino H, Mori KJ. 1989. Reproducible establishment of hemopoietic supportive stromal cell lines from murine bone marrow. Exp Hematol, 17 (2):145-153.

Jetani H, Garcia-Cadenas I, Nerreter T, Thomas S, Rydzek J, Meijide JB, Bonig H, Herr W, Sierra J, Einsele H, Hudecek M. 2018. CAR T-cells targeting FLT3 have potent activity against FLT3(-)ITD(+) AML and act synergistically with the FLT3-inhibitor crenolanib. Leukemia, 32 (5):1168-1179.

Juliusson G, Hough R. 2016. Leukemia. Prog Tumor Res, 43:87-100.

Kennedy VE, Smith CC. 2020. FLT3 Mutations in Acute Myeloid Leukemia: Key Concepts and Emerging Controversies. Front Oncol, 10:612880.

Krupka C, Kufer P, Kischel R, Zugmaier G, Bogeholz J, Kohnke T, Lichtenegger FS, Schneider S, Metzeler KH, Fiegl M, Spiekermann K, Baeuerle PA, Hiddemann W, Riethmuller G, Subklewe M. 2014. CD33 target validation and sustained depletion of AML blasts in long-term cultures by the bispecific T-cell-engaging antibody AMG 330. Blood, 123 (3):356-365.

Krupka C, Kufer P, Kischel R, Zugmaier G, Lichtenegger FS, Kohnke T, Vick B, Jeremias I, Metzeler KH, Altmann T, Schneider S, Fiegl M, Spiekermann K, Bauerle PA, Hiddemann W, Riethmuller G, Subklewe M. 2016. Blockade of the PD-1/PD-L1 axis augments lysis of AML cells by the CD33/CD3 BiTE antibody construct AMG 330: reversing a T-cell-induced immune escape mechanism. Leukemia, 30 (2):484-4

Lange B, Valtieri M, Santoli D, Caracciolo D, Mavilio F, Gemperlein I, Griffin C, Emanuel B, Finan J, Nowell P, et al. 1987. Growth factor requirements of childhood acute leukemia: establishment of GM-CSF-dependent cell lines. Blood, 70 (1):192-199.

Madduri D, Dhodapkar MV, Lonial S, Jagannath S, Cho HJ. 2019. SOHO State of the Art Updates and Next Questions: T-Cell-Directed Immune Therapies for Multiple Myeloma: Chimeric Antigen Receptor-Modified T Cells and Bispecific T-Cell-Engaging Agents. Clin Lymphoma Myeloma Leuk, 19 (9):537-544.

Marayati R, Quinn CH, Beierle EA. 2019. Immunotherapy in Pediatric Solid Tumors-A Systematic Review. Cancers (Basel), 11 (12).

Martin P, Papayannopoulou T. 1982. HEL cells: a new human erythroleukemia cell line with spontaneous and induced globin expression. Science, 216 (4551):1233-1235.

Maruta M, Ochi T, Tanimoto K, Asai H, Saitou T, Fujiwara H, Imamura T, Takenaka K, Yasukawa M. 2019. Direct comparison of target-reactivity and cross-reactivity induced by CAR- and BiTE-redirected T cells for the development of antibody-based T-cell therapy. Sci Rep, 9 (1):13293.

Matsuo Y, MacLeod RA, Uphoff CC, Drexler HG, Nishizaki C, Katayama Y, Kimura G, Fujii N, Omoto E, Harada M, Orita K. 1997. Two acute monocytic leukemia (AML-M5a) cell lines (MOLM-13 and MOLM-14) with interclonal phenotypic heterogeneity showing MLL-AF9 fusion resulting from an occult chromosome insertion, ins(11;9)(q23;p22p23). Leukemia, 11 (9):1469-1477.

Mestermann K, Giavridis T, Weber J, Rydzek J, Frenz S, Nerreter T, Mades A, Sadelain M, Einsele H, Hudecek M. 2019. The tyrosine kinase inhibitor dasatinib acts as a pharmacologic on/off switch for CAR T cells. Science Translational Medicine 11 (499):eaau5907.

Muller JP, Schmidt-Arras D. 2020. Novel Approaches to Target Mutant FLT3 Leukaemia. Cancers (Basel), 12 (10).

Munhoz RR, Postow MA. 2016. Recent advances in understanding antitumor immunity. F1000Res, 5:2545.

Myburgh R, Kiefer JD, Russkamp NF, Magnani CF, Nunez N, Simonis A, Pfister S, Wilk CM, McHugh D, Friemel J, Muller AM, Becher B, Munz C, van den Broek M, Neri D, Manz MG. 2020. Anti-human CD117 CAR T-cells efficiently eliminate healthy and malignant CD117-expressing hematopoietic cells. Leukemia, 34 (10):2688-2703.

Offner S, Hofmeister R, Romaniuk A, Kufer P, Baeuerle PA. 2006. Induction of regular cytolytic T cell synapses by bispecific single-chain antibody constructs on MHC class I-negative tumor cells. Mol Immunol, 43 (6):763-771.

Oiseth S, Aziz M. 2017. Cancer immunotherapy: a brief review of the history, possibilities, and challenges ahead. J Cancer Metastasis Treat (2017), 3:250-261.

Pelcovits A, Niroula R. 2020. Acute Myeloid Leukemia: A Review. R I Med J (2013), 103 (3):38-40.

Porter DL, Levine BL, Kalos M, Bagg A, June CH. 2011. Chimeric antigen receptor-modified T cells in chronic lymphoid leukemia. N Engl J Med, 365 (8):725-733.

Rieger MA, Schroeder T. 2012. Hematopoiesis. Cold Spring Harb Perspect Biol, 4 (12).

Rosnet O, Schiff C, Pebusque MJ, Marchetto S, Tonnelle C, Toiron Y, Birg F, Birnbaum D. 1993. Human FLT3/FLK2 gene: cDNA cloning and expression in hematopoietic cells Blood 82 (4):1110–1119.

Ross SL, Sherman M, McElroy PL, Lofgren JA, Moody G, Baeuerle PA, Coxon A, Arvedson T. 2017. Bispecific T cell engager (BiTE(R)) antibody constructs can mediate bystander tumor cell killing. PLoS One, 12 (8):e0183390.

Slaney CY, Wang P, Darcy PK, Kershaw MH. 2018. CARs versus BiTEs: A Comparison between T Cell-Redirection Strategies for Cancer Treatment. Cancer Discov, 8 (8):924-934.

Sommer C, Cheng HY, Nguyen D, Dettling D, Yeung YA, Sutton J, Hamze M, Valton J, Smith J, Djuretic I, Chaparro-Riggers J, Sasu BJ. 2020. Allogeneic FLT3 CAR T Cells with an Off-Switch Exhibit Potent Activity against AML and Can Be Depleted to Expedite Bone Marrow Recovery. Mol Ther, 28 (10):2237-2251.

Song W, Zhang M. 2020. Use of CAR-T cell therapy, PD-1 blockade, and their combination for the treatment of hematological malignancies. Clin Immunol, 214:108382.

Strohl WR, Naso M. 2019. Bispecific T-Cell Redirection versus Chimeric Antigen Receptor (CAR)-T Cells as Approaches to Kill Cancer Cells. Antibodies (Basel), 8 (3).

Subklewe M. 2021. BiTEs better than CAR T cells Blood advances, 5 (2):607–612.

Subklewe M, von Bergwelt-Baildon M, Humpe A. 2019. Chimeric Antigen Receptor T Cells: A Race to Revolutionize Cancer Therapy. Transfus Med Hemother, 46 (1):15-24.

Tabata R, Chi S, Yuda J, Minami Y. 2021. Emerging Immunotherapy for Acute Myeloid Leukemia. Int J Mol Sci, 22 (4).

Tsapogas P, Mooney CJ, Brown G, Rolink A. 2017. The Cytokine Flt3-Ligand in Normal and Malignant Hematopoiesis. Int J Mol Sci, 18 (6).

Wang X, Riviere I. 2016. Clinical manufacturing of CAR T cells: foundation of a promising therapy. Mol Ther Oncolytics, 3:16015.

Wang Y, Xu Y, Li S, Liu J, Xing Y, Xing H, Tian Z, Tang K, Rao Q, Wang M, Wang J. 2018. Targeting FLT3 in acute myeloid leukemia using ligand-based chimeric antigen receptor-engineered T cells. J Hematol Oncol, 11 (1):60.

Warmuth M, Kim S, Gu XJ, Xia G, Adrian F. 2007. Ba/F3 cells and their use in kinase drug discovery. Curr Opin Oncol, 19 (1):55-60.

Williams P, Basu S, Garcia-Manero G, Hourigan CS, Oetjen KA, Cortes JE, Ravandi F, Jabbour EJ, Al-Hamal Z, Konopleva M, Ning J, Xiao L, Hidalgo Lopez J, Kornblau SM, Andreeff M, Flores W, Bueso-Ramos C, Blando J, Galera P, Calvo KR, Al-Atrash G, Allison JP, Kantarjian HM, Sharma P, Daver NG. 2019. The distribution of T-cell subsets and the expression of immune checkpoint receptors and ligands in patients with newly diagnosed and relapsed acute myeloid leukemia. Cancer, 125 (9):1470-1481.

Yang H, Bueso-Ramos C, DiNardo C, Estecio MR, Davanlou M, Geng QR, Fang Z, Nguyen M, Pierce S, Wei Y, Parmar S, Cortes J, Kantarjian H, Garcia-Manero G. 2014. Expression of PD-L1, PD-L2, PD-1 and CTLA4 in myelodysplastic syndromes is enhanced by treatment with hypomethylating agents. Leukemia, 28 (6):1280-1288.

Yang Y. 2015. Cancer immunotherapy: harnessing the immune system to battle cancer. J Clin Invest, 125 (9):3335-3337.

Yang Y, Lin T, Jacoby E, Qin H, Gardner EG, Chien CD, Lee DW, Fry TJ. 2015 CD4 CAR T Cells Mediate CD8-like Cytotoxic Anti-Leukemic Effects Resulting in Leukemic Clearance and Are Less Susceptible to Attenuation By Endogenous TCR Activation Than CD8 CAR T Cells Blood, 126 (23).

Zhang P, Zhang C, Li J, Han J, Liu X, Yang H. 2019. The physical microenvironment of hematopoietic stem cells and its emerging roles in engineering applications. Stem Cell Res Ther, 10 (1):327.

Zieger N, Nicholls A, Wulf J, Hänel G, Pasikhani MK, Buecklein V, Brauchle B, Marcinek A, Nixdorf D, Rohrbacher L, Scheurer M, Kischel R, Spiekermann K, Weigert O, Theurich S, von Bergwelt M, Subklewe M. 2020. Treatment-Free Intervals Mitigate T-Cell Exhaustion Induced By Continuous CD19xCD3-BiTE® Construct Stimulation in Vitro Blood, 136 44–45.

9 List of Figures

10 List of Tables

11 Erklärung über die eigenständige Erstellung der Masterarbeit

Hiermit erkläre ich, dass ich die vorliegende Masterarbeit selbständig verfasst und keine anderen als die angegebenen Quellen und Hilfsmittel benutzt habe.

Die Stellen der Masterarbeit, die anderen Quellen im Wortlaut oder dem Sinn nach entnommen wurden, sind durch Angaben der Herkunft kenntlich gemacht. Dies gilt auch für Skizzen und bildliche Darstellungen.

_____ _____

Ort, Datum Helena Stadler